CONTEMPORARY REVIEW

Structure and function of the ventricular tachycardia isthmus

Edward J. Ciaccio, PhD,*† Elad Anter, MD,‡ James Coromilas, MD,§ Elaine Y. Wan, MD, FHRS,* Hirad Yarmohammadi, MD, FHRS,* Andrew L. Wit, PhD,¶ Nicholas S. Peters, MD, PhD, FHRS,† Hasan Garan, MD*

*From the *Department of Medicine, Division of Cardiology, Columbia University College of Physicians and Surgeons, New York, New York, †ElectroCardioMaths Programme, Imperial Centre for Cardiac Engineering, Imperial College London, London, United Kingdom, ‡Department of Cardiovascular Medicine, Cardiac Electrophysiology, Cleveland Clinic, Cleveland, Ohio, §Department of Medicine, Division of Cardiovascular Disease and Hypertension, Rutgers University, New Brunswick, New Jersey, and ¶Department of Pharmacology, Columbia University College of Physicians and Surgeons, New York, New York.*

Catheter ablation of postinfarction reentrant ventricular tachycardia (VT) has received renewed interest owing to the increased availability of high-resolution electroanatomic mapping systems that can describe the VT circuits in greater detail, and the emergence and need to target noninvasive external beam radioablation. These recent advancements provide optimism for improving the clinical outcome of VT ablation in patients with postinfarction and potentially other scar-related VTs. The combination of analyses gleaned from studies in swine and canine models of postinfarction reentrant VT, and in human studies, suggests the existence of common electroanatomic properties for reentrant VT circuits. Characterizing these properties may be useful for increasing the specificity of substrate mapping techniques and for noninvasive identification to guide ablation. Herein, we describe properties of reentrant VT circuits that may assist in elucidating the mechanisms of onset and maintenance, as well as a means to localize and delineate optimal catheter ablation targets.

KEYWORDS Catheter ablation; Isthmus; Mapping; Reentrant circuit; Ventricular tachycardia

(Heart Rhythm 2022;19:137–153)

Introduction

Ventricular tachycardia (VT) is an important clinical problem in patients with structural heart disease, including ischemic and nonischemic cardiomyopathies.[1–4] These patients are at increased risk for sustained ventricular tachyarrhythmias that can lead to hemodynamic decompensation including sudden cardiac death.[5] The primary mechanism of VT in these patients is reentry, also known as reentrant excitation, due to the continuous excitation of the ventricle during the entire cardiac cycle. Ablation procedures that have been used to identify and eliminate VT circuits can vary significantly depending on the substrate and the strategy for treatment. In some subgroups (post-myocardial infarction [post-MI] with slow and mappable VT), the results are excellent. Failure, when it occurs, tends to be related to limited mapping specificity when identifying VT isthmus sites critical for maintenance of the circuit.[6–8]

Major challenges for procedural improvement during VT ablation include the following. (1) The majority of VTs are hemodynamically unstable, preventing mapping of the circuit. (2) The substrate forming the VT isthmus is partially functional and may not be readily identified during sinus rhythm. (3) Ablation strategies to selectively eliminate areas forming isthmus sites have not been well established, particularly in large areas of scar with multiple exit sites. (4) VT circuits may be endocardial, epicardial, endo–epicardial, or intramural. Herein, our discussion shall be limited to reentrant VT in patients with ischemic cardiomyopathy, for which animal and human data on mechanism and electrical–structural correlation are most robust.

In structural heart disease, the primary mechanism of VT is reentry located within scar regions.[9,10] After MI, healing of the damaged tissue involves fibrogenesis that produces geometrically constrained formations of surviving,

Funding Sources: Dr Peters acknowledges funding for data analysis from the British Heart Foundation (RG/16/3/32175 and Centre of Research Excellence), Rosetrees Trust, and the National Institute for Health Research (UK) Biomedical Research Centre. Dr Wan acknowledges funding for data analysis from the National Institutes of Health, R01HL152236. Disclosures: Dr Anter has received research grants and consultation fees from Biosense Webster, Inc. He also receives research grants and consultation fees from Affera Inc, Boston Scientific, Itamar Medical, and Phillips Health. All other authors have reported that they have no relationships relevant to the contents of this paper to disclose. **Address reprint requests and correspondence:** Dr Edward J. Ciaccio, Columbia University, HP 7-729, 180 Fort Washington Ave, New York, NY 10032. E-mail address: ciaccio@columbia.edu.

1547-5271/ https://doi.org/10.1016/j.hrthm.2021.08.001

electrically conducting myocardial cells at infarct border zones[11] as well as wall thinning,[12] both of which affect the electrical activation pattern in the heart. The border zone characteristics depend on the location and duration of coronary occlusion as well as the reperfusion therapy.[13] The fibrogenesis component represents a pathologic remodeling of the myocardium, and it can be detected using certain types of cardiac imaging. Fibrosis separates myocyte bundles serving as conducting channels so that the activation wavefront takes a zigzag route with slowed conduction.[14,15] During premature stimulation, zones of denser fibrosis are associated with conduction delay.[16] Studies have found a positive correlation between the total scar mass and risk for VT.[17]

VT circuit pathways are frequently established within thin surviving tissue structures, several millimeters thick, surrounding the scar.[18] Although mapping of the VT circuit is the gold standard to identify its components including the targets of ablation, this is not possible in a large proportion of patients due to hemodynamic instability. Therefore, methods for identifying critical components of the VT circuit during stable rhythms, so-called substrate mapping, often are attempted.[19] Substrate mapping is implemented during stable sinus or paced rhythm to identify the VT targets.[20,21] The underlying principle governing the process of substrate mapping is that the bundles of surviving myocytes within heterogeneous scar that are identified during sinus rhythm may form VT isthmuses.[22] However, successful activation mapping with ablation of VT remains a challenging task because conditions present during VT may not be present during stable rhythms, in part due to the difficulty in precisely identifying crucial properties of the VT circuit, as well as the influence of the variation in activation wavefront orientation on how the ventricular scar is characterized.[23]

A reentrant circuit is an electrical pathway along which the activation wavefront travels in a loop or loops, having a circular pattern.[24] Each repeat excursion of the impulse around the circuit defines a cycle of VT. The isthmus, which is also known as the diastolic corridor or central common pathway, is a protected segment in the circuit where all loops rejoin, and ablation at this location has the best chance to disrupt the circuit. In order to better localize reentrant circuits and optimize ablation strategies, it would be useful to describe the circuit structure and function. Recognizing the characteristics during high-density substrate mapping could assist in more rapid detection of arrhythmogenic regions for more efficacious catheter ablation during electrophysiological (EP) study. Herein, the properties common to many reentrant VTs are described and discussed, with schematic diagrams used for illustration.

Circuit morphology

The shape of the VT circuit can exhibit several patterns (Figure 1). In the case of the single-loop form, the electrical activation wavefront, noted by arrows, propagates around a lone area of inexcitability (Figure 1A). There can be an isthmus, for example, where the mitral annulus may act to constrain the circuit, as shown.[10] Such a single-loop isthmus has an entrance and an exit. For the double-loop circuit, also known as a figure-of-8, there are 2 areas of inexcitability

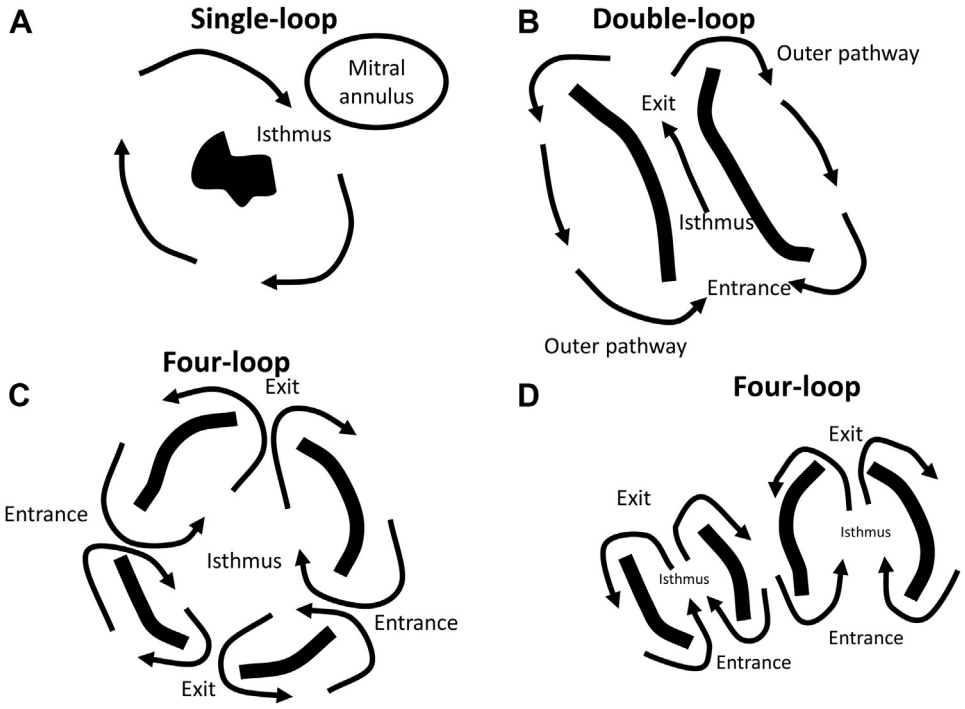

Figure 1 Forms of the reentrant circuit. In each case, the activation wavefront *(arrows)* travels around inexcitable regions **A:** Single-loop configuration. **B:** Double-loop or figure-of-8. **C:** Four-loop. **D:** Alternate form for 4-loop with 2 isthmuses.

(Figure 1B). Propagation of the wavefront around the double-loop proceeds through the isthmus, which is the narrow region common to both circuit loops, as shown. The time during which it propagates through the isthmus occurs during the diastolic interval of the electrocardiogram (ECG), that is, the interval between the end of the QRS wave of one beat of VT and the beginning of the QRS wave of the next.[25,26] At the isthmus exit, the impulse bifurcates, the 2 wavefronts travel around areas of inexcitability in the outer pathway, they coalesce, and then reenter the previously excited area (shown). Some circuits with a double-loop appearance are actually maintained by the shorter dominant loop, rather than by both loops.[27] Occasionally a 4-loop reentrant circuit pattern has also been observed, but thus far only in rabbit and in canine postinfarction hearts.[28–31] When the 4-loop circuit has a single isthmus, it is a region common to all 4 loops with at least 2 entrances and 2 exits (Figure 1C). The wavefronts propagate around 4 areas of inexcitability, as depicted. Two distinct isthmuses may also communicate to form 4 loops overall (Figure 1D).

In clinical studies of patients following MI, activation mapping has demonstrated the presence of a reentrant circuit which can be composed of a single loop.[10,32–35] The inexcitable region may be formed by an aneurysm,[32] a functional, transverse arc of block in parallel to muscle fiber axis,[34] or an anatomic line of block.[35] Double-loop reentrant circuits are also frequently observed in clinical studies,[4,10,33,35–40] and the isthmus lateral boundaries tend to be partially or mostly comprised of functional arcs of conduction block,[10,22,23,33–37,39,40–46] although anatomic components may be present as well. Many such reentrant circuits have 2 or more entrances or exits, as well as dead ends and bystander regions.[1,4,10,26,39,43,47–50]

In animal models, as in clinical cases, single-loop circuits occur,[51–54] and double-loop forms are frequently observed,[1,29,51,52,54–57] whereas, as aforementioned, 4-loop patterns are sometimes evident.[28–31] Some reentrant circuits in postinfarction canine hearts are also transmural, involving both midmyocardial and heart surface components.[58]

Circuit conductive properties

The entrance to and exit from the isthmus are circuit regions where conduction slowing can occur, while conduction within the isthmus itself can have near-normal properties.[1] Reentrant circuits often appear exclusively at the endocardial or epicardial heart surface,[38,59] but they also can be located midmyocardially. For midmyocardial circuits, the pathway is 3-dimensional, but this can only be appreciated when both epicardial and endocardial mapping are performed.[40] Recent high-density mapping studies have shown that some circuits are transmural, involving endocardial, midmyocardial, and epicardial pathways.[40,60]

In canine 3-to 5-day postinfarction experiments, in part because there is no fibrotic scarring,[52,55,61,62] functional block is apparent at the lateral isthmus boundaries,[51–53,56,63] although, in about one-third of cases, anatomic block is also manifest along short segments of these boundaries.[31] In older canine infarcts, anatomic block often corresponds to patches of dense scar.[58] Propagation of the wavefront as observed in sinus rhythm activation maps suggests that reentrant circuits in swine postinfarction are also largely determined by functional rather than fixed anatomic barriers.[64]

The formation of functional block is dependent on heterogeneities of the EP properties of myocardial fibers.[65] It can occur as a result of the remodeling of gap junctions and ion channel properties[66] or with changes in wavefront direction due to source–sink (impedance or current-to-load) mismatch.[30,67–75] An arc of conduction block can be considered to be functional if it appears during reentrant VT but not during sinus rhythm[31] or pacing. It can be considered to be anatomic if it is present during sinus rhythm, pacing, and VT.[31] However, these definitions are not exact, as anatomic block will not be apparent if the activation wave travels in parallel to it or intercepts at an oblique angle. Indeed, in postoperative mapping, it has been observed that a transverse block line observed during sinus rhythm may disappear and be replaced by a smooth spread of activation at the onset of programmed stimulation.[34] Functional block has also been defined as an area of myocardium that is not electrically excitable at shorter coupling intervals but is excitable at relatively long cycle lengths.[51] A broad definition of functional block would be that electrical conduction block occurs in some circumstances of wavefront orientation and coupling interval, but not all. Anatomic block would then be defined as an area resulting from anatomic defect where conduction block occurs regardless of wavefront orientation and coupling interval, although its appearance can be masked when the wavefront travels in parallel or intercepts at oblique angles.

From clinical noncontact mapping analysis, sustained reentry is more common in circuits having greater dimension of isthmus length and width, whereas nonsustained (or transient) VT, defined as being <30 seconds in duration, tends to occur when isthmus dimensions are reduced.[36] Nonsustained episodes are also more common when the entrance and exit points to the isthmus are narrower, and when the difference in sinus rhythm activation time across them is relatively large, so as to form electrical discontinuities.[29,36] The reentrant circuit dimensions that are characteristic of a particular postinfarction heart can be identified by pace mapping[76]; however, this sometimes overestimates isthmus size.[1]

Anisotropy refers to the anatomic and biophysical properties of the myocardium, which vary with direction.[65] Normal conduction velocity of the activation wavefront in the myocardium is anisotropic—it is faster in the longitudinal vs the transverse fiber direction. In canine postinfarction, the ratio has been found to be approximately 1.6:1.[66] Due to remodeling of ion channel and gap junctional connections between myocytes, the conduction velocity in canine postinfarction slows in both the longitudinal and transverse directions at the outer pathway, which is the portion of the reentrant circuit outside the isthmus. Here, slowing is more prominent in the transverse direction, so the anisotropic ratio

becomes 2:1.[66] Within the isthmus itself, conduction velocity is slowest, but with the anisotropic ratio returning to 1.6:1. Conduction velocity typically slows further at turning points at the isthmus entrance and exit due to changes in wavefront curvature,[1,56] with conduction velocity ranging from 0.10 to 15 mm/ms there, which greatly contributes to the overall tachycardia cycle length. In canine postinfarction, cycle length tends to prolong with larger dimensions of isthmus length and width, when the circuit pathway lengthens, and when there is a narrowed isthmus segment leading to a sharp distal expansion,[77] which can result in additional wavefront slowing at the distal end due to impedance mismatch.[67–71,77–79] Likewise, in swine postinfarction, there is a direct dependence of tachycardia cycle length on isthmus length and width.[80] Larger dimensions of length and width have been shown to correlate with the presence of multiple circuit loops,[29] as well as with multiple isthmus entrance and/or exit points.[29,36] In clinical studies, VT cycle length is at least partially correlated to conduction velocity along the outer circuit loop.[35,81]

Central isthmus electrogram morphology

The isthmus of the reentrant circuit was first shown to overlap a thinnest layer of surviving infarct border zone in a canine postinfarction model of VT.[55,61,63] At the isthmus location, heart wall thinning is evident in clinical studies.[82,83] The characteristic has implications for the morphology of electrograms acquired from the region. In human VT, midisthmus electrogram deflections are typically low in voltage.[1,10,23,39,76,82,84–87] Based on the formulation of the extracellular signal, the thinness of the viable myocardium is directly responsible for the diminished amplitude observed in the electrogram deflections because of the decreased volume of activating myocytes.[84,88,89] Central or midisthmus electrograms also tend to be relatively short in duration.[88] Short electrogram deflections are indicative of a faster activation wavefront.[88] Although the wavefront is slowed overall in the infarct border zone and in the circuit,[66] the isthmus long axis tends to orient approximately in parallel to muscle fibers,[77] in which direction the wavefront conduction velocity is fastest, which would account for the faster speed observed there during VT. Late potentials recorded at the midisthmus have a lower amplitude and shorter duration compared to bystander sites, and they are predictive of location.[35,90,91] Where slow conduction is evident at turning points, electrograms are also low in voltage and long in duration due to the reduced velocity.[35] Both VT and sinus rhythm low-voltage electrograms have been used to empirically guide a standard ablation catheter toward the isthmus,[59,92–94] although these electrogram features are not always specific to the isthmus region.

The low-voltage characteristic of electrograms acquired from the isthmus is consistent with the observation that dense scar overlaps these recording sites.[10,20,87] Because scar tissue is completely unexcitable when only a very small number of myocytes are present in the scar that forms the isthmus, the electrograms generated will exhibit a particularly low voltage level.[86] However, scar and the thinness of the surviving region are not the only factors contributing to the low electrogram voltage; substrate remodeling in the form of gap junction and ion channel alteration is also important to consider.[1] The overall diminished voltage levels generated when the isthmus activates are such that the diastolic interval of VT, during which diastolic electrogram potentials are generated,[85] does not significantly contribute to ECG signal deflections.[76,95] The diastolic potentials of VT, which are defined as any distinct electrogram components inscribed after the surface QRS complex, partially correspond to locations of late potentials observed during sinus rhythm.[96] However, the absence of sinus rhythm late potentials does not guarantee the absence of arrhythmogenic pathways.[97] In canine postinfarction, sinus rhythm electrograms at the midisthmus location are low in amplitude, they tend to be short in duration, and they can also be biphasic.[98]

Examples of central isthmus electrogram formation and characteristics are illustrated in Figure 2, with activation maps indicative of the direction of wavefront propagation from early to late (colors from red to violet). The observed properties are in agreement with the mechanism of extracellular signal generation in myocardial tissue.[88] In Figure 2A, the bipolar electrode is denoted by circled symbols (+ and –). Here the electrogram is of low amplitude in a region of thin border zone (left side). Elsewhere in the infarct border zone, the viable tissue is thicker (right side), such that when the wavefront propagates, at any particular time epoch a larger volume of tissue activates, thereby generating a larger-amplitude electrogram. Isthmus electrograms recorded with a bipolar electrode often are narrow, indicating that the wavefront tends to be moving relatively rapidly.[88] This is depicted by the travel direction (arrow) and narrow electrogram in Figure 2B (left side). However, elsewhere in the circuit, if the wavefront were to be traveling less rapidly and therefore along a lesser distance per unit time, due, for example, to being conducted more transversely with respect to muscle fibers,[66] the resulting electrogram deflection would be wider (Figure 2B, right side).

Central isthmus bipolar electrograms can be biphasic.[98] Thus, as the wavefront propagates along the viable thin slab (Figure 2C, left side), it first arrives at the positive electrode, generating a positive electrogram deflection, and then at the negative electrode, generating a negative deflection.[88] The biphasic shape of the electrogram suggests that the wavefront is traveling through viable tissue directly beneath the bipolar recording electrode, rather than being recorded as a far-field effect. If, instead, the electrode were distant from the electrically activating tissue in the configuration shown (Figure 2C, right side) a far-field activation sequence would produce a uniphasic deflection, with the amplitude of the single deflection dependent on the distance between bipolar electrode pair and the activating tissue. However, electrogram shape is not always indicative of near- vs far-field activation, and it can only serve as an approximate guide toward isthmus location.

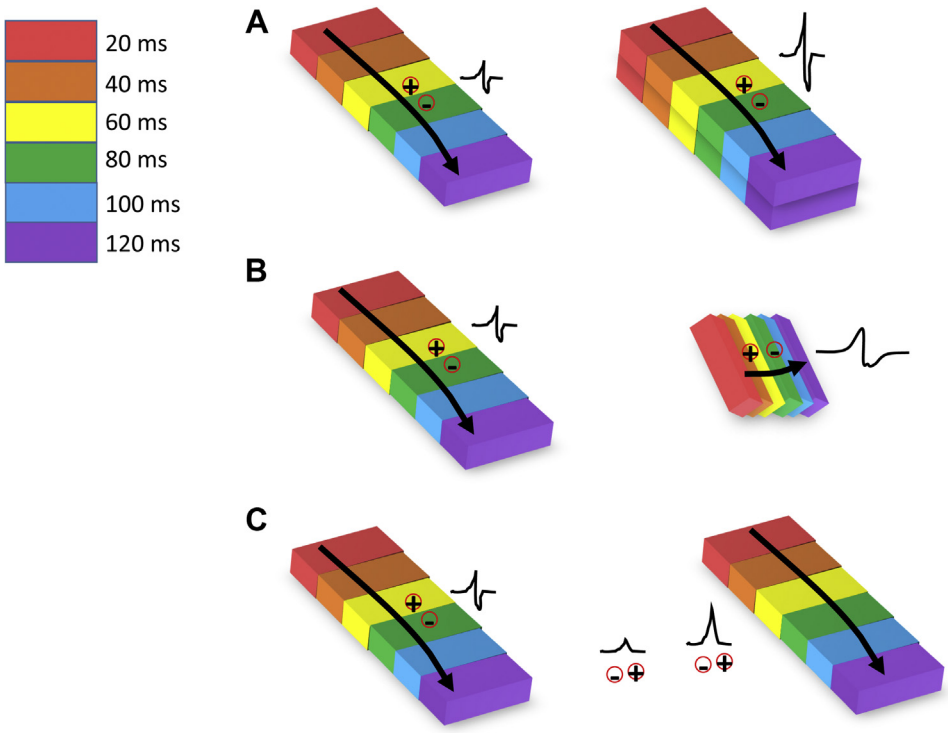

Figure 2 Isthmus electrograms tend to be low in amplitude, narrow, and biphasic. *Red* to *violet* denotes early to later activation times. **A:** When a thinner slab of tissue activates **(left)**, the resulting electrogram is low amplitude **(left)**. However when a thicker slab of tissue activates **(right),** it produces a larger electrogram. **B:** When wavefront propagation is rapid, a narrow electrogram is generated **(left)**. Yet, for slower propagating wavefronts **(right)**, the resulting electrogram is wide. **C:** When the electrogram is biphasic **(left)**, it suggests that wavefront propagation is directly beneath the electrode **(left)**. However, a uniphasic deflection with an amplitude dependent on location **(right)** indicates a far-field source.

Lateral isthmus boundary electrogram morphology

Fractionated electrograms can be defined as either 2 discrete deflections separated by an isoelectric interval (double potentials or split deflections) or an electrogram comprising many components.[61] They are more commonly observed in patients with reentrant VT than in patients without inducible arrhythmia.[99,100] Fractionation occurs where poorly coupled myocardium is present at regions with myocardial disarray, often due to the proximity of fibrous tissue interspersed with myocyte bundles.[41,61,101] Thus, wherever dense scar is identified, fractionated electrograms are often present within or at adjacent areas.[102] It also can occur wherever there is electrical discontinuity, whether due to current-to-load mismatch or differing excitability of coupling characteristics.[103] Although fractionation may be evident at any abnormal heart region, computer modeling suggests that it is more associated with the edges of dense scar.[104] In human VT, very slow conduction with associated long fractionated electrograms often are present at the lateral isthmus boundaries.[1,10,39,105] In canine postinfarction VT as well, electrograms acquired along lines of functional block at isthmus lateral boundaries tend to be of long duration and fractionated.[52,75,89] Based on the sharp change in border zone thickness there and the resulting impedance mismatch, fractionation can appear at these locations during sinus rhythm as well as during VT.[89,98] In canine postinfarction, temporal changes in fractionated electrogram shape, and therefore alterations in the slow discontinuous wavefront propagation pattern from which they are generated, are evident at the boundaries during both VT and sinus rhythm.[106,107] In both clinical and canine VT, fractionation at the lateral boundaries becomes more pronounced when the wavefront impinges from the perpendicular direction.[89,105]

Should portions of the main activation wavefront of the circuit begin to propagate across the lateral isthmus boundaries when they are composed of functional conduction block, they would travel slowly enough so that breakthrough does not ordinarily occur.[10,39] Such traversal-going wavefronts are stopped by the main wavefront as it swings around the outer pathway to the other side of the circuit loop.[1,29,36] Wherever fractionated electrograms are demonstrated in healed canine infarcts, the conduction velocity may decrease to as low as 0.04 mm/ms.[61] This degree of slowness would preclude wavefront breakthrough across the lateral boundaries at typical VT cycle lengths, due to the quicker return of the main wavefront to the other side of the boundary. Hence, outward at the boundaries, although functional block often is evident, in actuality, very slow wavefront propagation may be proceeding across.[29,89] Due to anisotropic conduction, when the wavefront travel direction across the boundaries is transverse to myocardial fibers, there is additional slowing, further supporting the maintenance of the reentrant circuit.[52] Yet, breakthrough across the boundaries

can, in fact, occur should the VT cycle length substantially prolong.[36] The presence of wavefront propagation in different directions on opposite sides of a boundary line has been termed pseudoblock.[108]

A schematic diagram of the electrical discontinuity that can be present at the lateral isthmus boundaries is shown in Figure 3. The main wavefront of the circuit (labeled mw) propagates along the isthmus long axis and tends to be longitudinally conducted with respect to muscle fibers, but other components of the wave tend to be transversely conducting across the lateral boundaries (labeled tc). A small area of the boundary is shown magnified, with the enlarged map depicting early activation in red and latest activation in violet. In Figure 3A (right side), the wavefront propagates rapidly in segment α, propagates somewhat more slowly in segment β, and propagates very slowly in segment δ. Thus, the wavefront becomes discontinuous, in accordance with generation of the extracellular signal.[88] The bipolar electrode from which the electrogram is acquired is noted by black circles in proximity to the center of the slab (Figure 3A, right side). At the early fast segment labeled α, the first electrogram deflection is generated, labeled deflection α (Figure 3A, top left). This deflection is narrow and early because the wavefront travels rapidly through segment α with little delay. The segment with intermediate wavefront speed, segment β, is responsible for generation of deflection β, which is wider and later because the wavefront is slower. The very slow segment, segment δ, is the source of deflection δ, which is very wide, very late, and also of low amplitude because it is furthest away from the bipolar electrode. Thus, fractionation occurs. When conduction block forms at the boundary line (Figure 3B, gray area in enlarged section at right), it can also be a source of discontinuity and electrogram fractionation. The activation wavefront propagates around it and initially produces deflection α. Then the negative deflections are generated (β and δ) as the wavefront travels in the opposite direction. Hence, at isthmus boundaries, both wavefront slowing (Figure 3A) and wavefront block (Figure 3B) can result in discontinuous conduction, and these phenomena are sources of electrogram fractionation.[89]

Multiple reentrant VT morphologies—Isthmus characteristics

Many patients with ischemic heart disease and VT have episodes of reentry with differing QRS morphologies that either occur spontaneously[42,109,110] or are inducible by programmed stimulation.[36,109–112] Single premature stimuli can result in induction of multiple reentrant VT morphologies, and more aggressive stimulus protocols can result in additional morphologies.[109–112] Patients with multiple VT morphologies are less likely to have successful ablation treatment outcomes.[113–115] This probably reflects a more complex arrhythmia substrate in patients with failed ablation.[115] Limited, thinnest portions of the infarct border zone are capable of forming stable lines of block forming isthmus boundaries that are supportive of reentrant VT.[55,63,72] The same areas can serve as anchor points for wavefront slowing and curvature events that occur in each of the multiple possible reentrant VT morphologies,[22,56,80,116] and the presence of tissue heterogeneity at such locations is an important property of the underlying substrate.[56,117,118] Similar properties of multiple reentrant VT morphologies have been observed in a canine postinfarction model.[119]

Predicting the multiple reentrant VT morphologies that will form in a particular patient is of interest for improving treatment strategy. Differences in VT morphologies may result from changes in entrance and exit points along the isthmus,[36,39,120] wavefront propagation around differing lines of block, or wavefront propagation around the same lines of block in opposite directions.[1,31,119] There is often an approximate but not precise overlap of lateral, functional

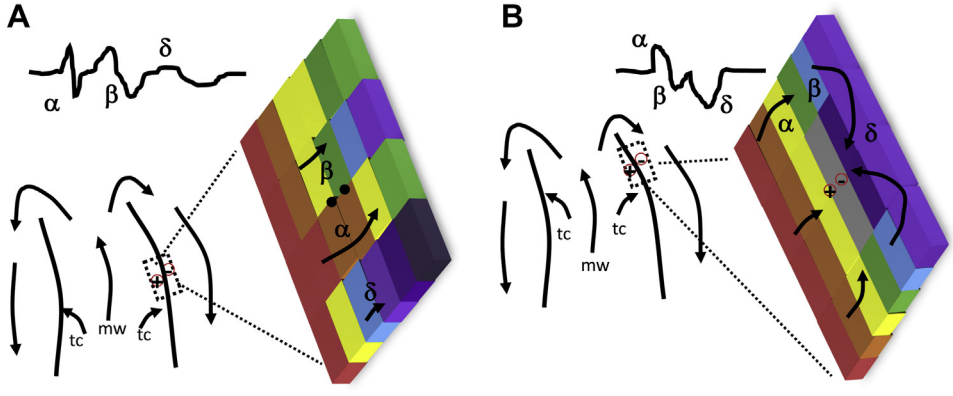

Figure 3 Fractionation at the isthmus boundaries is caused by discontinuous conduction, with an electrical activation wavefront that slows or blocks. In each panel, simulated electrograms are shown at **top**, propagation through the reentry isthmus is illustrated at **left**, and the magnified isthmus edge is illustrated in colors at **right**. The symbols α, β, and δ are used to label distinct electrogram deflections and also the corresponding wavefront location at the magnified area of isthmus border. The main wavefront in the reentry isthmus is labeled as mw; transversely conducting wavefronts are labeled tc. **A:** Disparities in the degree of wavefront conduction velocity cause electrical discontinuity at the magnified isthmus edge, resulting in electrogram fractionation. **B:** Presence of conduction block causes other wavefront dissociation, also causing fractionation.

block lines for 2 reentrant circuit morphologies in which the wavefront travels in opposite directions during the diastolic interval.[31] The variations between circuit morphologies due to changes in functional block are related to the programmed stimulus location, the coupling interval between stimuli, and the cycle length of VT.[30,36]

In both human and in animal postinfarction studies, it is rare for multiple VT circuit morphologies to reside in differing regions of the heart.[109,119,121] However, patients with multiple infarctions, in whom the total infarct size is large, are more likely to have multiple spontaneously occurring tachycardia morphologies, which can arise at distinct locations as measured by clinical criteria.[109,110,119,121] In such cases, each of multiple areas where wall thinning is observed could be likely sources of the disparate reentrant circuits.

Related to the occurrence of multiple morphologies in VT is the presence of pleomorphism. Precise definitions of these factors would be as follows. Pleomorphism is the occurrence of VT with more than 1 QRS morphology during the same episode. The cause of pleomorphic VT is often an alteration in the lateral isthmus boundaries with a resulting varied exit route.[35,43,119,120,122] In postinfarction patients with pleomorphic, hemodynamically stable VT, a shared isthmus is present in almost one-half of patients.[123] Multiple morphology can be defined as the occurrence of VT with differing morphology in differing episodes.[124,125] However, some groups also refer to pleomorphism using the multiple morphology definition.

Role of transient conduction block in the isthmus for reentry onset

Reentrant circuits are initiated by the presence of slow conduction and unidirectional block when there is a sufficient pathlength around inexcitable areas.[8,24,30,42,43,46,51,61,63,71,73,75,104,114,117,126–131] At VT onset, a transient line of unidirectional block forms in response to spontaneous or stimulated premature excitation,[30,34,36,37,42,73-75,85,128,130] or from rapid ventricular pacing.[32] Some possible mechanisms by which unidirectional block occurs include differences in activation wavefront propagation with respect to fiber orientation due to nonuniform anisotropy, which causes differences in conduction velocity,[132] discontinuities in axial resistance leading to decremental conduction,[133] heterogeneous refractory periods of action potentials with different repolarization,[117] disparities in the recovery of excitability,[129] and impedance mismatch.[30,72–75]

Reentry of the activation wavefront through the unidirectional block line into previously excited tissue occurs when the length of the circuit (ie, the pathlength) equals or exceeds the wavelength, which is defined as the product of the wavefront conduction velocity and the tissue refractory period.[134] Onset of the anisotropic form of reentry, which is frequently observed in VT, is characterized by conduction block in the transverse direction, due in part to reduced transverse conductivity, with successful conduction in the longitudinal direction.[1,22,52,56,62,64,66,101,117,135–138] A reduction in transverse conductivity leads to slowed conduction transverse to muscle fibers.[138–140] Yet, the reentry isthmus does not always align with muscle fibers.[77] The isthmus can be oriented off-axis to muscle fibers, and it can even be aligned transversely.[77] Hence, other mechanisms must also be at work in the formation of functional block at lateral boundaries.

Examples of VT induction success and failure are depicted in Figure 4. This schematic emphasizes that for reentry to occur, the premature stimulus site and the resulting lines of block are constrained to specific locations. The stimulus site is noted by a top-hat symbol in each panel. When a programmed premature stimulus is applied during sinus rhythm, unidirectional block does not occur at the isthmus location shown in Figures 4A–4C; therefore, reentrant VT is not inducible for any of these configurations. When there is a long coupling interval between successive stimuli, each stimulus-driven wavefront propagates through the region without blocking (Figure 4A). However, there may be inexcitable areas as shown by dashed lines (ie, the lateral isthmus boundaries during VT [structural or functional]). Similarly, when the stimulus site is within the isthmus location and the programmed stimulus has a long coupling interval (Figure 4B), although conduction block may be evident at the lateral boundaries, the wavefronts can travel around and extinguish. Were the stimulus site to reside in the outer pathway (Figure 4C), whether at a long or a short stimulus coupling interval, block may again occur, but the wavefronts extinguish, this time within the isthmus region. In the lower panels, however, conditions by which reentry can be initiated via programmed stimulation are shown. The stimulus site may be approximately aligned with the isthmus long-axis, either outside (Figure 4D) or within the isthmus (Figure 4E). When stimuli have a short coupling interval, less than the VT cycle length, conduction block can occur within the isthmus. When unidirectional block forms there (dotted line), the wavefront bifurcates, 2 distinct wavefronts travel around the line of block, they coalesce, and proceed in the opposite direction (Figures 4D and 4E). The electrical impulse thus propagates through the entranceway of what can be termed the protoisthmus (ie, the nascent isthmus) from the opposite direction, and, if there is time for recovery of excitability, onset of reentry occurs.

Wherever the stimulus site is located, to cause unidirectional block, the stimulated wavefront should arrive at the area where block will form from an approximately perpendicular (normal) direction.[71] Although the stimulus may originate from any location in the left or right ventricle, wavefront arrival from an approximately perpendicular direction probably is more likely if the stimulus site is aligned and in proximity to the protoisthmus exit (shaded region in Figure 5A). Anywhere in the entire gray shaded region with the stimulus mark shown would therefore be expected to serve as an optimal location to cause reentry induction. Too far skewed from the long-axis, however, and the stimulus wavefront would not as likely impinge at the unidirectional block line

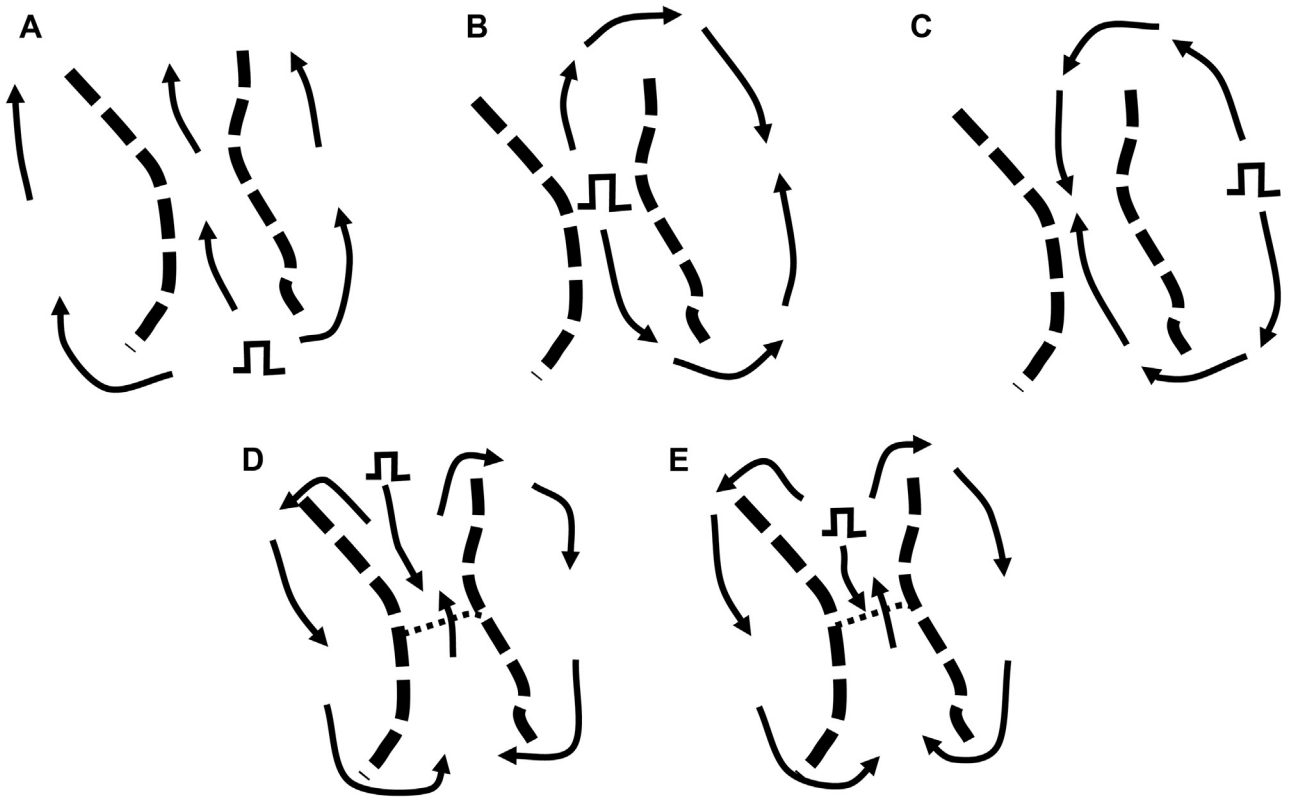

Figure 4 Unidirectional block is needed to initiate reentrant ventricular tachycardia (VT) and depends on stimulus site location and coupling interval. **A–C:** Unsuccessful induction of VT. **D, E:** Successful induction of VT.

location from an approximately perpendicular direction. Too far away, and the wavefront might become discontinuous and no longer rectilinear when it arrives at the unidirectional block line location. When the stimulus site is more distant, 2 or 3 premature impulses may be useful to reduce the intervening refractory period so that the wavefront can reach the protoisthmus early enough to cause block. If the conditions for premature stimulus site location are met, then the unidirectional block line can form (Figure 5B), the remaining portions of the wavefront bifurcate and coalesce, and reentry proceeds (Figure 5C).

Impedance mismatch is one possible mechanism for the formation of the unidirectional block line leading to reentry.[30,73–75] This depends on changes in border zone thickness, as illustrated in Figure 5D. The thinnest border zone occurs throughout the isthmus location and reaches a minimum in proximity to the position where the unidirectional block line will form (noted in Figure 5D as thin). With the stimulus site at the area shown, the premature stimulus wavefront will suddenly encounter thinnest-to-thicker tissue. Functional block will form if the coupling interval of the premature stimulus is sufficiently short and if the thinnest region is on the order of 500 μm or less in thickness.[30,73–75] Encountering the region for thin-to-thicker tissue, the wavefront becomes concave in shape, resulting in an insufficient electric current available in the forward direction for propagation of the activation wavefront to continue. Therefore, the wavefront would bifurcate, travel around as distinct wavefronts, and reenter (Figures 5B and 5C).

Besides the restrictions on stimulus properties and the thinness of the viable substrate, the range of isthmus size for which reentry is inducible is also constrained. It is limited at the lower end by the need for a sufficient pathlength to maintain an excitable gap at the wavefront leading edge.[56,71,75,77,131] It is limited at the high end by the longest pathlength that will not be interrupted by a sinus escape beat[75,77] or by breakthrough along the path.[75]

Three-dimensionality of the isthmus in reentrant circuits

Although originally thought of and diagrammed as being 2-dimensional, the reentry isthmus must be constrained in 3 dimensions. Because a majority of reentrant VTs are hemodynamically unstable and not well tolerated, this precludes the performance of lengthy entrainment and activation mapping procedures for circuit characterization.[3,141,142] The differences in the circuit between patients with tolerated vs untolerated VT are not well understood,[50] so it is not possible to determine *a priori* which clinical VTs will be mappable with a standard catheter. However, high-resolution mapping technologies implemented in recent EP studies have been found useful in rapidly delineating reentrant circuit characteristics in patients,[40,99,143] as well as in swine[1,22,64,80,101,144] and canine models.[145] This mode enables isthmus

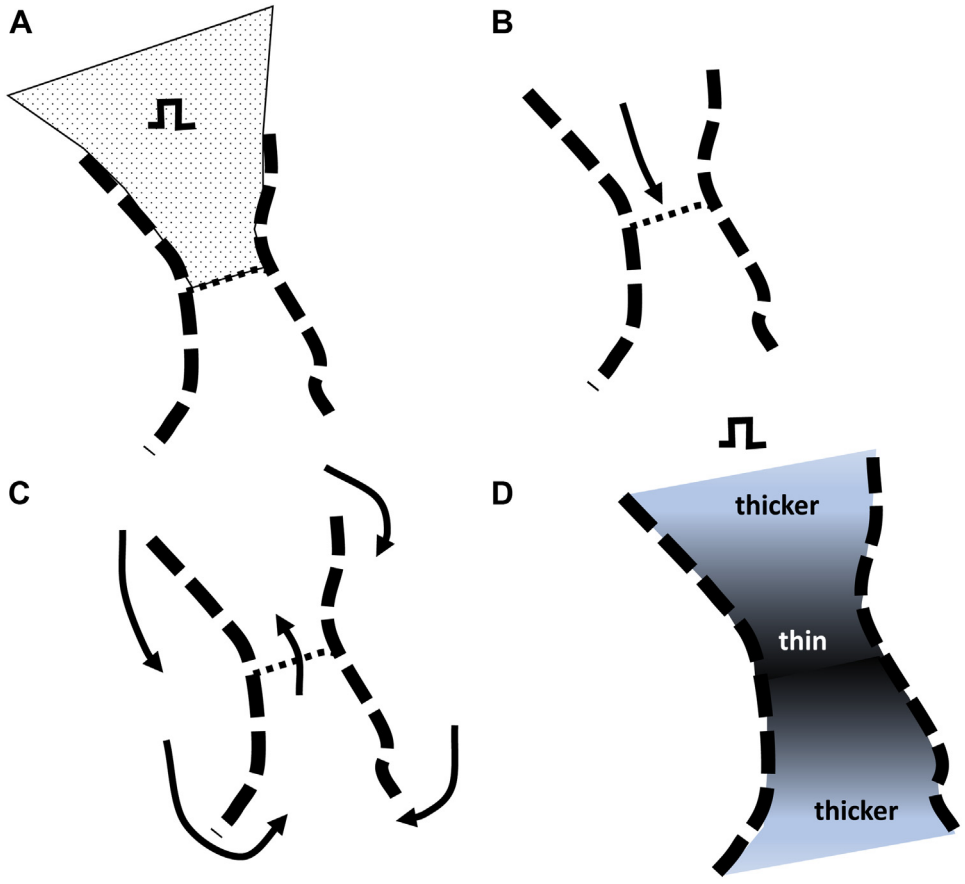

Figure 5 **A:** Range of optimal sites for premature stimulation leading to reentry onset is illustrated by the *gray shaded area*. **B:** Premature stimulation. **C:** Ventricular tachycardia induction. **D:** Infarct border zone—changes in thickness of viable substrate that are necessary for unidirectional block to occur by impedance mismatch.

dimensions, and the extent of the exit region recorded on both endocardial and epicardial surfaces, to be estimated with precision and speed.[40] Based on such analyses, some circuits in clinical studies have been found to activate in a thin layer restricted to a single myocardial surface.[36,114,146] However, reentry at depth, with either nonuniform transmural propagation, or with focal activation patterns apparent at heart surfaces that are consistent with the presence of midmyocardial reentry, are also frequently observed.[40,42,147] In such instances, epicardial or endocardial surface mapping alone would fail to demonstrate a complete reentrant circuit because the activation pathway may involve both surfaces as well as intramural sites.[40,42,148] Intramural location of the VT isthmus is a recognized cause for endocardial or epicardial ablation failure.[148] Recordings from needle electrodes have been found useful for substrate mapping of intramural VT and for selecting ablation targets to interrupt the circuit.[149] In canine postinfarction with midmyocardial reentry components, the circuit can be completed by incorporating local electrograms recorded from intramural sites with the surface electrogram activation sequence.[58] In such instances, VT is reproducibly terminated by selectively rendering intramural sites refractory with extrastimuli, critically timed to activate during the excitable gap.[58]

Imaging technologies are becoming increasingly relevant for characterizing 3-dimensional left ventricular structure, three-dimensional scar, and the border zone substrate.[150] The development of imaging parameters for the quantification of edema, infarction and scar has been followed by their adoption for non-invasive tissue characterization in acute and chronic MI.[151] Late gadolinium enhancement enables the direct quantification of the spatial extent of scar[5,151–154] and myocardial fibrosis,[17,155] and it is predictive of fibrosis[156] and risk of arrhythmia.[7,118,157–159] Based on imaging technology, wall-thinning has been shown to colocalize with voltage-defined scar.[150,160] Areas with severe wall thinning noted in the imagery may be indicative of denser scar, which act as zones of conduction block, while VT isthmuses may reside in channels of relatively preserved thickness within the scar.[83] The spatial resolution of cardiac computed tomography is on the order of 1 millimeter or less.[5,150,161] Similar spatial resolutions are achieved with cardiac magnetic resonance imaging.[162]

Recently, myocardial calcifications have been detected by cardiac computed tomography in postinfarction patients and have been shown to be associated with VT.[161] Such calcifications are not electrically excitable, so they represent an anatomic boundary for reentrant circuits. Areas of

calcifications have been found to be effective ablation sites in more than one-third of postinfarction VT patients.[161]

Reentrant circuits as viewed at high resolution in 3 dimensions can appear in many varied forms. However, all of these forms are distillable into a few basic patterns.[74,75] When a reentrant circuit is located at depth, it must be bounded at the isthmus or around the entire circuit (Figure 6). Figure 6A shows the general pattern when it is constrained only at the isthmus. The excitable area is depicted in blue, and the activation wavefront enters and exits from all sides in 3 dimensions. Inexcitable tissue bordering the isthmus is illustrated by gray color, and there may be inexcitable tissue in the periphery as well. The reentry isthmus itself is the constrained region in 3 dimensions. Within the midmyocardium, the circuit may also be completely constrained around a single loop (Figure 6B).[74,75] Within this loop, composed of a bundle of myocytes, or channel, there is excitable tissue, but outside and around it, and perhaps elsewhere in proximity to the midmyocardial region, there is inexcitable tissue (gray). The entire circuitous channel is therefore the isthmus in Figure 6B. For onset of reentry for either of the cases shown in Figures 6A and 6B, a bulge or dilation formed by an increase in the diameter of the channel because of the presence of additional myocytes can lead to unidirectional block by impedance mismatch (smaller-to-larger volume of viable tissue) (Figure 6C).[73–75] The aperture along the conduit increases dramatically from left to right, causing unidirectional block at short coupling intervals (dotted line). However, if the wavefront travels from right to left (Figure 6D), there is no such dramatic increase in aperture, which is required for functional block to form, only a gradual increase, and the wavefront therefore persists.

Although it is evident that reentrant circuits at depth are 3-dimensional, reentry must also be constrained in 3 dimensions when present at a heart surface.[30,72,75] Consider the area that forms the isthmus at a surface as depicted in Figure 7B. The viable tissue is shown by colors, with activation from early to late noted by red to violet colors. The wavefront, when traveling along the subendocardium, is constrained above by the heart chamber and beneath by the nonconducting infarct (termed the no-flux condition), which is shown in black color. This structural configuration appears, for example, in postinfarction reentrant VT regions when measured by cardiac magnetic resonance imaging or by histologic analysis.[55,63,72] The infarct area typically forms an approximately trapezoidal shape along the isthmus long-axis in 3 dimensions (Figure 7B, black area).[30,72–75,89] Therefore, near and at the surface where viable conducting tissue is present, toward the center of the isthmus, the surviving layer is thinnest (also see Figure 5D).

In the surface configuration, functional block can occur at the lateral boundaries during reentry. Several mechanisms may be responsible, which include changes in ion channel and gap junctional properties[55,56,66] as well as impedance mismatch.[30,72,75] With regard to impedance mismatch, wherever there is a sufficiently thin volume of electrically activating tissue, with the wavefront propagating outward to a distal expansion of viable tissue, slowing or block will occur when the coupling interval for activation is relatively short, as described earlier for other configurations. This region of

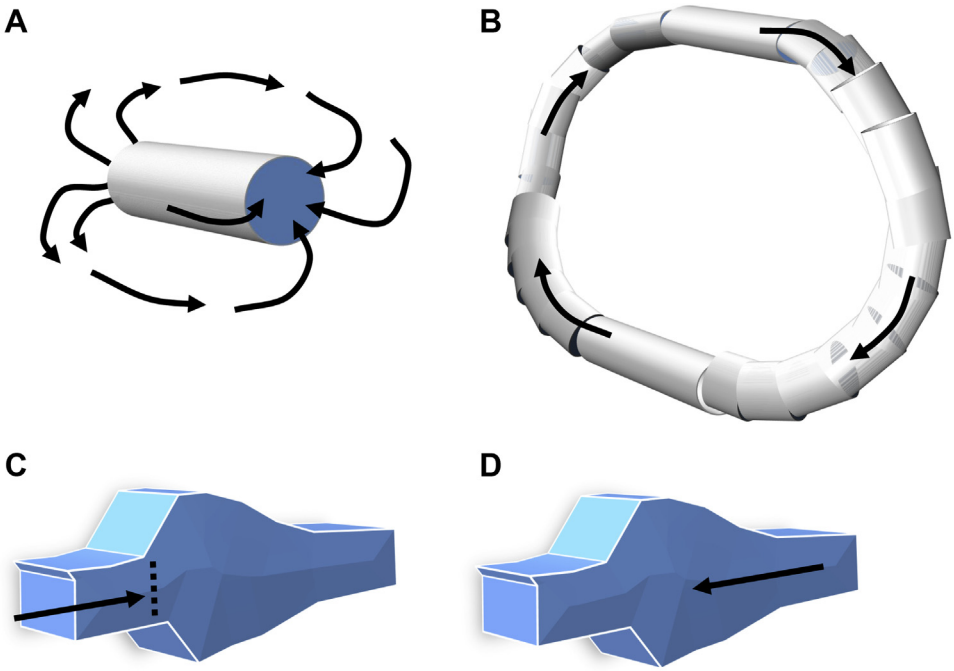

Figure 6 The isthmus must be constrained in 3 dimensions and can be midmyocardial. **A:** Isthmus is constrained. **B:** The entire circuit is constrained. *Arrows* indicate the direction of activation wavefront propagation during ventricular tachycardia. **C:** Unidirectional block of the activation wavefront can occur at short programmed stimulus coupling intervals where there is a sharp distal expansion in the channel. **D:** In the opposite direction, there is no such sharp distal expansion, and the propagating activation wavefront will not block.

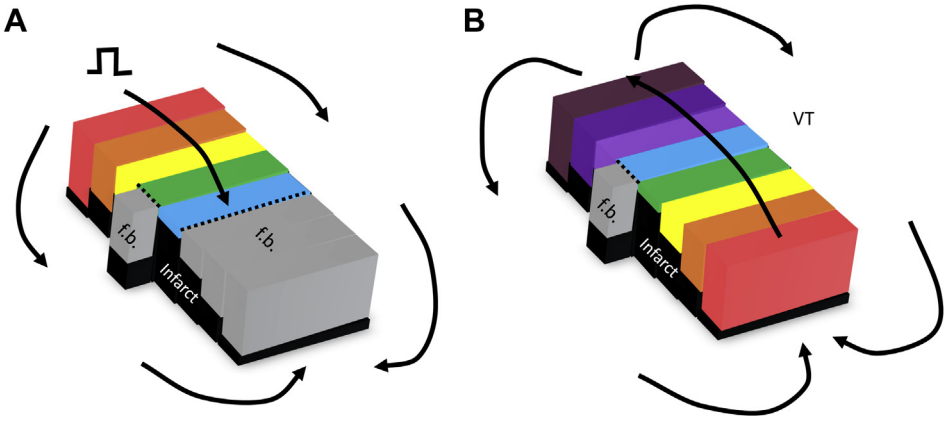

Figure 7 The isthmus must be constrained in 3 dimensions and can be at the heart surface. **A:** Premature stimulation leading to reentry onset. **B:** Reentrant ventricular tachycardia (VT). *Arrows* indicate direction of wavefront propagation. The wavefront blocks at the edges of *gray areas* because of the sharply increased distal expansion in the direction of travel. f.b. indicates *gray areas* that do not electrically activate because of functional block.

distal expansion is noted in gray in Figure 7B. When activation occurs at the very thin region denoted by blue color, there is insufficient current to excite the much thicker gray area; thus, functional block is manifested at the boundary (dotted line). Although only a small segment where functional block forms is shown, according to the geometry it would actually be present along much of both lateral boundaries in Figure 7B. The electrical impulse must then propagate through the isthmus constrained to the direction of its long-axis, whereupon at the exit it bifurcates, travels around, and coalesces.

To induce reentry for this 3-dimensional surface configuration, a premature stimulus is needed (Figure 7A). The coupling interval must be very short, with activation proceeding away from the stimulus site (top-hat symbol). As aforementioned, at very short coupling intervals the wavefront can block at the thin-to-thicker viable tissue, the interface between blue and large gray areas in the central isthmus (Figure 7A, longer dotted line), as well as at the lateral boundaries where there is a sharper thickness change (Figure 7A, shorter dotted line).[30,75,89] Hence, the wavefront must propagate around, and it can then enter the isthmus region from the other side (ie, at the protoisthmus entrance). If there is time for recovery of excitability, onset of reentry occurs. The circuit then perpetuates at the longer cycle length of reentry without blocking in the isthmus (Figure 7B).

Current technology for mapping and ablation of circuit morphologies

Ablation of VT is dependent on locating the diastolic activity (ie, the isthmus region), which is critical for maintenance of the reentrant circuit.[3] Bipolar voltage mapping is often utilized as a gold standard for electroanatomic scar delineation during VT ablation procedures.[163] It can be helpful to characterize all clinically relevant VT circuits during EP study to improve ablation outcome.[141] However, decreased recurrence of multiple VT morphologies can also be achieved with recently developed strategies involving extensive homogenization of the substrate, as it represents a probabilistic approach for transecting key limbs of a reentrant circuit.[8,164–167] Furthermore, utilizing functional information based on wavefront propagation to identify areas of abnormal activation has been shown to be valuable.[8]

Specifically targeting low-voltage electrogram sites can eliminate reentrant VT.[59,168] Yet, the definition of a normal left ventricular endocardial voltage in patients with postinfarct scar is still lacking.[169] The values of bipolar electrogram cutoffs are also limited by activation wavefront direction,[170] and there are significant voltage differences between diagonally orthogonal bipolar electrode pairs at any given recording site.[171] High-density multielectrode grid catheters can offer improvement because they enable simultaneous recordings from multiple orthogonal directions with the ability to select the largest voltage level in a small region[170,172] and can improve depiction of the diastolic pathway.[173] Extensive substrate ablation of local abnormal ventricular activity (LAVA) evident during sinus rhythm or pacing is also utilized in targeting.[164,174] LAVA can be defined as a sharp, high-frequency ventricular potential that is distinct from a preceding or overlapping far-field deflection.[164] When extrastimuli with decreasing coupling intervals are applied from the right ventricular apex, LAVAs can be observed to progressively split further away from the far-field component. Therefore, they are poorly coupled to the rest of the myocardium and are considered to be indicative of local electrical activity arising from damaged tissue.

To the present time, the success rate for VT ablation diminishes when multiple tachycardia morphologies are inducible.[20,168] Furthermore, endocardial voltage mapping has a limited ability to detect midmyocardial or epicardial scar.[150] Because mapping and ablation of multiple target regions can be difficult, many patients have recurring episodes after initial treatment, and they must undergo repeat procedures, which increase morbidity and may lead to malignant tachycardias.[20,168] Although many reentrant circuit locations are associated with endocardial scar, some are linked with epicardial scar as well.[40,59,94,175,176] Therefore, mapping of

both endocardial and epicardial surfaces can improve the efficacy of ablation procedures when the circuit is not localized to 1 heart surface.[40,59] The detection of midmyocardial or subepicardial scar by magnetic resonance scanning is helpful to identify patients who are likely to require epicardial mapping for successful abolition of VT.[177,178] Cardiac imaging and mapping techniques have recently been used to identify targets for noninvasive external beam radioablation.[179] Thus it may be possible to develop a completely noninvasive method for VT ablation.

Many clinical EP ablation procedures are based on sinus rhythm activation mapping and analysis.[180] Measurements of conduction velocity during sinus rhythm can provide functional and structural insight into the initiation and perpetuation of arrhythmia.[181] The isthmus long-axis is often aligned with the principal direction of wavefront propagation during sinus rhythm.[35,45,98,116] After infarction, the region in proximity to the isthmus, which is remodeled,[62,66] exhibits slow and uniform conduction during sinus rhythm, as is observed in both clinical studies and in canine and swine postinfarction.[22,31,36,80,98,116,182] The slowing can result from alterations in conduction properties, from fibrosis, and/or from changes in collagen texture.[66,183] During EP study, regions with steep activation slowing during normal sinus rhythm are predictive of VT termination sites.[184] Targeting of slow conduction regions propagating into late activation is also a promising strategy for substrate modification.[22,31,36,80,98,116] However, this strategy largely accounts for isthmus sites that are formed by fixed anatomic barriers and usually correspond to bipolar voltage amplitude $<$0.5 mV. Yet, because of the nonuniform anisotropic tissue properties, isthmus sites may form in other areas with seemingly normal conduction during sinus rhythm. These may be revealed by stimulation from different directions or coupling intervals.[23] Furthermore, ablation strategies guided by elimination of all areas of steep activation slowing as identified during sinus rhythm and stimulation of the LV from different directions has resulted in improved clinical outcomes compared to ablation at sites of activation slowing during sinus rhythm alone. The ability to identify surrogates during sinus rhythm to localize arrhythmogenic regions may further improve as the relationship between scar wavefront propagation patterns and abnormal electrograms becomes clearer.[8]

Myocardial regions with late or fractionated sinus rhythm potentials are abnormal, but not all such areas coincide with the VT diastolic pathway.[185] If an extrastimulus originating from the right ventricle significantly delays onset of these features, they are termed decrement evoked potentials.[185,186] The position of the substrate from which they are acquired has been found to colocalize with the VT diastolic pathway, and, after its ablation, ischemic cardiomyopathy patients exhibited a lower incidence of VT recurrence.[185,186] Similarly, right ventricular extrastimulation during sinus rhythm can be used to elicit evoked conduction delay of low-voltage near-field potentials.[187] Ablation of this substrate in post-MI patients with small or nontransmural scar improves outcome.

When multiple VT morphologies can be elicited by programmed stimulation during EP study, sinus rhythm mapping suggests that there can be a common anchor point, centered at a region with late activation.[22,36,80,116] The direction of propagation through each isthmus during reentry parallels a direction proceeding away from the anchor point, where sinus rhythm activation is late (serving as the isthmus entrance area), toward regions with early sinus rhythm activation (serving as the isthmus exit area).[22,31,36,80,98,116] The anchor, being late-activating during sinus rhythm, may stabilize the pathway from which stimuli can initiate multiple reentrant circuit morphologies that begin at the common point.[22,80] Tissue properties at the region of late sinus rhythm activation would be expected to be abnormal so that activation there is more likely to be delayed during premature excitation, serving to initiate VT.[22,80,116]

Future directions for mapping and ablation of circuit morphologies

The benefit of catheter ablation in reentrant VT patients with structural heart disease is well known, with freedom from recurrence approaching 70%.[188] However, the success rate with this procedure has plateaued, despite advances in both mapping catheter technology and electroanatomic mapping systems.[188,189] High-density, multielectrode catheters can enhance the possibility of detailed activation mapping of even poorly tolerated VTs because they can be produced in a reasonable time frame. It has recently been shown that in patients with a fully mappable diastolic pathway recording, after an ablative procedure there is higher freedom from VT recurrence.[188] In such circumstances, creating a transecting ablation line to target the narrowest isthmus where the electrical impulse is most constrained can be used to prevent VT reinduction with minimized patient risk. Yet, even with advanced techniques, complete VT isthmus mapping is unachievable in several circumstances,[188] such as (1) progressive hemodynamic deterioration requiring pace termination; (2) catheter-induced termination with inability to reinduce the clinical VT; (3) presence of an intramural substrate; and (4) presence of an epicardial substrate in cases where epicardial access is contraindicated. The contraindications for epicardial access include pericarditis, femoral pseudoaneurysm, and cardiac tamponade.[188] When VT isthmus mapping is incomplete, if diastolic activity is missing on the endocardial surface, epicardial mapping may provide the missing link to record the entire diastolic pathway. When no compete diastolic pathway is evident, substrate-guided ablation has become the method of choice to guide procedures. The ablation strategies that have been developed include scar homogenization, scar dechanneling, targeting zones of isochronal crowding, elimination of near-field activity, and elimination of late potentials at sites of conduction slowing during sinus rhythm,[188,189] although efficacy is limited. Moreover, ablation success is in part dependent on the indicator used, such as contact force and impedance drop, which are imperfect measures to determine the irreversible loss of cellular

excitability needed to interrupt the circuit by myocardial heating with temperatures >50°C.[189]

Although not yet realized, there is the potential for a well-placed ablation lesion no more than several centimeters across to abolish all inducible VTs in patients,[92] and this has been shown in canine[31,98,119] and swine[118] postinfarction models. A recently developed technique termed core isolation may prove useful for eliminating all possible VT morphologies that can occur, although it involves more extensive ablation.[102,189] It is performed by defining the putative isthmus and early exit sites. Areas of dense scar with the presence of low-amplitude electrograms are the criteria used to define the core region. After core elements of the VT circuit are identified, they can then be ablated circumferentially with the goal of achieving electric isolation.[102] Successful isolation of the core is then demonstrated by exit block from within the entire isolated region.

Practical implications and recommendations for the clinical electrophysiologist

With the advent of rapid, high-resolution mapping, it is possible to speed the process for discerning the arrhythmogenic region where the reentrant VT isthmus forms and then to ablate across the area where the wavefront is constrained during the diastolic interval in order to interrupt the circuit. The several paradigms for targeting ablation sites as described herein may become more efficacious in preventing VT reinduction when used with high-resolution mapping technology, which streamlines information-gathering so that a decision on where and how to ablate can may be rapidly made. Yet, there is a need for improved interpretation of endocardial and epicardial activation maps arising from a midmyocardial or transmurally situated reentrant circuit. There is also a need to improve technologies for the actual mapping of such circuits in clinical patients. Based on both computer modeling and clinical observations, the narrowest isthmus is an ideal point to ablate in patients with single VT morphologies. Finding this region may involve the detection and use of areas of conduction slowing during sinus rhythm as a preliminary guide. How to best ablate substrates in which multiple clinical reentrant morphologies are inducible is undetermined as yet and is an important area for future research efforts.

Summary and conclusion

Treatment of postinfarction VT caused by a reentrant circuit is an important clinical problem in which the electrical conduction pathway must be interrupted to prevent reinduction of arrhythmia. Early as well as ongoing studies in canine and swine animal models are generally supportive of clinical findings in regard to this topic. The properties common to many reentrant circuits are manifold. Typically, a single- or double-loop pattern is observed. Bipolar electrograms recorded from within the central isthmus region tend to be low in voltage, narrower in width, and biphasic, whereas at the lateral isthmus boundaries and at points of wavefront turning, fractionated electrograms with longer duration are more commonly observed. These electrogram properties may be useful for targeting arrhythmogenic zones with ablation energy during substrate mapping. Increasing the accuracy of substrate mapping, however, may require stimulation at different locations with a variety of coupling intervals to more closely simulate the VT activation pattern.[190] For reentrant VT induction, a short premature stimulus coupling interval and unidirectional block are needed, with the stimulus site location usually being toward the protoisthmus exit. Depending on stimulus site location and coupling interval, there is the possibility that multiple reentrant circuit morphologies may arise from a common origin due to the presence of structural heterogeneity. Although reentrant circuits typically are diagrammed as being 2-dimensional, the isthmus is, in fact, 3-dimensionally constrained, whether it forms midmyocardially or at a heart surface, or is transmural. Functional block can form lateral isthmus boundaries when there is a sharp change from thinnest to thicker border zone or in response to alterations in ion channel and gap junctional properties. Anatomic lines of block may arise and form parts or all of the lateral isthmus boundaries wherever there is substantial fibrosis or calcification.

References

1. Anter E, Tschabrunn CM, Buxton AE, Josephson ME. High-resolution mapping of postinfarction reentrant ventricular tachycardia: electrophysiological characterization of the circuit. Circulation 2016;134:314–327.
2. Martinez BK, Baker WL, Konopka A, et al. Systematic review and meta-analysis of catheter ablation of ventricular tachycardia in ischemic heart disease. Heart Rhythm 2020;17:e206–e219.
3. Schilling RJ, Peters NS, Davies DW. Simultaneous endocardial mapping in the human left ventricle using a noncontact catheter: comparison of contact and reconstructed electrograms during sinus rhythm. Circulation 1998;98:887–898.
4. Stevenson WG. Ventricular tachycardia after myocardial infarction: from arrhythmia surgery to catheter ablation. Cardiovasc Electrophysiol 1995; 6:942–950.
5. Mahida S, Sacher F, Dubois R, et al. Cardiac imaging in patients with ventricular tachycardia. Circulation 2017;136:2491–2507.
6. Williams ES, Viswanathan MN. Current and emerging antiarrhythmic drug therapy for ventricular tachycardia. Cardiol Ther 2013;2:27–46.
7. Tang PT, Do DH, Li A, Boyle NG. Team management of the ventricular tachycardia patient. Arrhythm Electrophysiol Rev 2018;7:238.
8. Aziz Z, Tung R. Novel Mapping strategies for ventricular tachycardia ablation. Curr Treat Options Cardiovasc Med 2018;20:34.
9. Hsia HH, Lin D, Sauer WH, Callans DJ, Marchlinski FE. Anatomic characterization of endocardial substrate for hemodynamically stable reentrant ventricular tachycardia: identification of endocardial conducting channels. Heart Rhythm 2006;3:503–512.
10. Martin R, Maury P, Bisceglia C, et al. Characteristics of scar-related ventricular tachycardia circuits using ultra-high-density mapping: a multi-center study. Circ Arrhythm Electrophysiol 2018;11:e006569.
11. Gyöngyösi M, Winkler J, Ramos I, et al. Myocardial fibrosis: biomedical research from bench to bedside. Eur J Heart Fail 2017;19:177–191.
12. Shah DJ, Kim HW, James O, et al. Prevalence of regional myocardial thinning and relationship with myocardial scarring in patients with coronary artery disease. JAMA 2013;309:909–918.
13. Buja LM. Myocardial ischemia and reperfusion injury. Cardiovasc Pathol 2005; 14:170–175.
14. de Bakker JM, van Capelle FJ, Janse MJ, et al. Slow conduction in the infarcted human heart. 'Zigzag' course of activation. Circulation 1993;88:915–926.
15. Stevenson WG. Ventricular scars and ventricular tachycardia. Trans Am Clin Climatol Assoc 2009;120:403.

16. Kawara T, Derksen R, de Groot JR, et al. Activation delay after premature stimulation in chronically diseased human myocardium relates to the architecture of interstitial fibrosis. Circulation 2001;104:3069–3075.
17. Shiozaki AA, Senra T, Arteaga E, et al. Myocardial fibrosis detected by cardiac CT predicts ventricular fibrillation/ventricular tachycardia events in patients with hypertrophic cardiomyopathy. J Cardiovasc Comput Tomogr 2013; 7:173–181.
18. Pashakhanloo F, Herzka DA, Halperin H, McVeigh ER, Trayanova NA. Role of 3-dimensional architecture of scar and surviving tissue in ventricular tachycardia: insights from high-resolution ex vivo porcine models. Circ Arrhythm Electrophysiol 2018;11:e006131.
19. Bourier F, Martin R, Martin CA, et al. Is it feasible to offer 'targeted ablation' of ventricular tachycardia circuits with better understanding of isthmus anatomy and conduction characteristics? Europace 2019;21(Suppl 1):i27–i33.
20. Marchlinski FE, Callans DJ, Gottlieb CD, Zado E. Linear ablation lesions for control of unmappable ventricular tachycardia in patients with ischemic and nonischemic cardiomyopathy. Circulation 2000;101:1288–1296.
21. Reddy VY, Neuzil P, Taborsky M, Ruskin JN. Short-term results of substrate mapping and radiofrequency ablation of ischemic ventricular tachycardia using a saline-irrigated catheter. J Am Coll Cardiol 2003;41:2228–2236.
22. Anter E, Kleber AG, Rottmann M, et al. Infarct-related ventricular tachycardia: Redefining the electrophysiological substrate of the isthmus during sinus rhythm. JACC Clin Electrophysiol 2018;4:1033–1048.
23. Anter E, Neuzil P, Reddy VY, et al. Ablation of reentry-vulnerable zones determined by left ventricular activation from multiple directions: a novel approach for ventricular tachycardia ablation: a multicenter study (PHYSIO-VT). Circ Arrhythm Electrophysiol 2020;13:e008625.
24. Mines GR. On circulating excitation in heart muscles and their possible relation to tachycardia and fibrillation. Trans R Soc Can 1914;8:43–52.
25. Fitzgerald DM, Friday KJ, Wah JA, Lazzara R, Jackman WM. Electrogram patterns predicting successful catheter ablation of ventricular tachycardia. Circulation 1988;77:806–814.
26. Stevenson WG, Khan H, Sager P, et al. Identification of reentry circuit sites during catheter mapping and radiofrequency ablation of ventricular tachycardia late after myocardial infarction. Circulation 1993;88:1647–1670.
27. Nishimura T, Upadhyay GA, Aziz ZA, et al. Double loop ventricular tachycardia activation patterns with single loop mechanisms: asymmetric entrainment responses during "pseudo-figure-of-eight" reentry. Heart Rhythm 2021 May. 7:S1547-5271(21)00419-7.
28. Lin SF, Roth BJ, Wikswo JP. Quatrefoil reentry in myocardium: an optical imaging study of the induction mechanism. J Cardiovasc Electrophysiol 1999; 10:574–586.
29. Ciaccio EJ. Ventricular tachycardia duration and form are associated with electrical discontinuities bounding the core of the reentrant circuit. J Cardiovasc Electrophysiol 2005;16:646–654.
30. Ciaccio EJ, Coromilas J, Wit AL, Peters NS, Garan H. Source-sink mismatch causing functional conduction block in re-entrant ventricular tachycardia. JACC Clin Electrophysiol 2018;4:1–6.
31. Ciaccio EJ, Coromilas J, Wan EY, et al. Slow uniform electrical activation during sinus rhythm is an indicator of reentrant VT isthmus location and orientation in an experimental model of myocardial infarction. Comput Methods Progr Biomed 2020;196:105666.
32. Miller JM, Harken AH, Hargrove WC, Josephson ME. Pattern of endocardial activation during sustained ventricular tachycardia. J Am Coll Cardiol 1985; 6:1280–1287.
33. Downar E, Harris L, Mickleborough LL, Shaikh N, Parson ID. Endocardial mapping of ventricular tachycardia in the intact human ventricle: evidence for reentrant mechanisms. J Am Coll Cardiol 1988;11:783–791.
34. Downar E, Harris L, Kimber S, et al. Ventricular tachycardia after surgical repair of tetralogy of Fallot: results of intraoperative mapping studies. J Am Coll Cardiol 1992;20:648–655.
35. Frontera A, Pagani S, Limite LR, et al. The outer loop and isthmus in ventricular tachycardia circuits: characteristics and implications. Heart Rhythm 2020; 17:1719–1728.
36. Ciaccio EJ, Chow AW, Kaba RA, Davies DW, Segal OR, Peters NS. Detection of the diastolic pathway, circuit morphology, and inducibility of human postinfarction ventricular tachycardia from mapping in sinus rhythm. Heart Rhythm 2008;5:981–991.
37. De Chillou C, Groben L, Magnin-Poull I, et al. Localizing the critical isthmus of postinfarct ventricular tachycardia: the value of pace-mapping during sinus rhythm. Heart Rhythm 2014;11:175–181.
38. de Chillou C, Sellal JM, Magnin-Poull I. Pace mapping to localize the critical isthmus of ventricular tachycardia. Card Electrophysiol Clin 2017; 9:71–80.
39. Martin R, Hocini M, Haïsaguerre M, Jaïs P, Sacher F. Ventricular tachycardia isthmus characteristics: insights from high-density mapping. Arrhythm Electrophysiol Rev 2019;8:54.
40. Tung R, Raiman M, Liao H, et al. Simultaneous endocardial and epicardial delineation of 3D reentrant ventricular tachycardia. J Am Coll Cardiol 2020; 75:884–897.
41. de Bakker JM, van Capelle FJ, Janse MJ, et al. Reentry as a cause of ventricular tachycardia in patients with chronic ischemic heart disease: electrophysiologic and anatomic correlation. Circulation 1988;77:589–606.
42. Pogwizd SM, Hoyt RH, Saffitz JE, Corr PB, Cox JL, Cain ME. Reentrant and focal mechanisms underlying ventricular tachycardia in the human heart. Circulation 1992;86:1872–1887.
43. Downar E, Saito J, Doig JC, et al. Endocardial mapping of ventricular tachycardia in the intact human ventricle. III. Evidence of multiuse reentry with spontaneous and induced block in portions of reentrant path complex. J Am Coll Cardiol 1995;25:1591–1600.
44. Chow AW, Schilling RJ, Davies DW, Peters NS. Characteristics of wavefront propagation in reentrant circuits causing human ventricular tachycardia. Circulation 2002;105:2172–2178.
45. Ciaccio EJ, Chow AW, Davies DW, Wit AL, Peters NS. Localization of the isthmus in reentrant circuits by analysis of electrograms derived from clinical noncontact mapping during sinus rhythm and ventricular tachycardia. J Cardiovasc Electrophysiol 2004;15:27–36.
46. Segal OR, Chow AW, Peters NS, Davies DW. Mechanisms that initiate ventricular tachycardia in the infarcted human heart. Heart Rhythm 2010;7:57–64.
47. Downar E, Kimber S, Harris L, et al. Endocardial mapping of ventricular tachycardia in the intact human heart. II. Evidence for multiuse reentry in a functional sheet of surviving myocardium. J Am Coll Cardiol 1992;20:869–878.
48. Tung R, Mathuria N, Michowitz Y, et al. Functional pace-mapping responses for identification of targets for catheter ablation of scar-mediated ventricular tachycardia. Circ Arrhythm Electrophysiol 2012;5:264–272.
49. Tung R, Shivkumar K. Unusual response to entrainment of ventricular tachycardia: in or out? Heart Rhythm 2014;11:725–727.
50. Tung R. Challenges and pitfalls of entrainment mapping of ventricular tachycardia: ten illustrative concepts. Circ Arrhythm Electrophysiol 2017; 10:e004560.
51. El-Sherif N, Smith RA, Evans K. Canine ventricular arrhythmias in the late myocardial infarction period. 8. Epicardial mapping of reentrant circuits. Circ Res 1981;49:255–265.
52. Dillon SM, Allessie MA, Ursell PC, Wit AL. Influences of anisotropic tissue structure on reentrant circuits in the epicardial border zone of subacute canine infarcts. Circ Res 1988;63:182–206.
53. Schoels W, Restivo M, Caref EB, Gough WB, El-Sherif N. Circus movement atrial flutter in canine sterile pericarditis model. Activation patterns during entrainment and termination of single-loop reentry in vivo. Circulation 1991; 83:1716–1730.
54. Cabo C, Schmitt H, Masters G, Coromilas J, Wit AL, Scheinman MM. Location of diastolic potentials in reentrant circuits causing sustained ventricular tachycardia in the infarcted canine heart: relationship to predicted critical ablation sites. Circulation 1998;98:2598–2607.
55. Peters NS, Coromilas J, Severs NJ, Wit AL. Disturbed connexin43 gap junction distribution correlates with the location of reentrant circuits in the epicardial border zone of healing canine infarcts that cause ventricular tachycardia. Circulation 1997;95:988–996.
56. Peters NS, Coromilas J, Hanna MS, Josephson ME, Costeas C, Wit AL. Characteristics of the temporal and spatial excitable gap in anisotropic reentrant circuits causing sustained ventricular tachycardia. Circ Res 1998;82:279–293.
57. Ciaccio EJ, Tosti AC, Scheinman MM. Method to predict isthmus location in ventricular tachycardia caused by reentry with a double-loop pattern. J Cardiovasc Electrophysiol 2005;16:528–536.
58. Garan H, Fallon JT, Rosenthal S, Ruskin JN. Endocardial, intramural, and epicardial activation patterns during sustained monomorphic ventricular tachycardia in late canine myocardial infarction. Circ Res 1987;60:879–896.
59. Soejima K, Stevenson WG, Sapp JL, Selwyn AP, Couper G, Epstein LM. Endocardial and epicardial radiofrequency ablation of ventricular tachycardia associated with dilated cardiomyopathy: the importance of low-voltage scars. J Am Coll Cardiol 2004;43:1834–1842.
60. Raiman M, Tung R. Automated isochronal late activation mapping to identify deceleration zones: rationale and methodology of a practical electroanatomic mapping approach for ventricular tachycardia ablation. Comput Biol Med 2018;102:336–340.
61. Gardner PI, Ursell PC, Fenoglio JJ Jr, Wit AL. Electrophysiologic and anatomic basis for fractionated electrograms recorded from healed myocardial infarcts. Circulation 1985;72:596–611.

62. Peters NS, Wit AL. Myocardial architecture and ventricular arrhythmogenesis. Circulation 1998;97:1746–1754.
63. Wit AL, Allessie MA, Bonke FI, Lammers W, Smeets J, Fenoglio JJ Jr. Electrophysiologic mapping to determine the mechanism of experimental ventricular tachycardia initiated by premature impulses. Am J Cardiol 1982; 49:166–185.
64. Tschabrunn CM, Roujol S, Nezafat R, et al. A swine model of infarct-related reentrant ventricular tachycardia: electroanatomic, magnetic resonance, and histopathological characterization. Heart Rhythm 2016;13:262–273.
65. Wit AL, Dillon SM, Coromilas J, Saltman AE, Waldecker B. Anisotropic reentry in the epicardial border zone of myocardial infarcts. Ann N Y Acad Sci 1990;591:86–108.
66. Cabo C, Yao J, Boyden PA, et al. Heterogeneous gap junction remodeling in reentrant circuits in the epicardial border zone of the healing canine infarct. Cardiovasc Res 2006;72:241–249.
67. Kogan BY, Karplus WJ, Billett BS, Stevenson WG. Excitation wave propagation within narrow pathways: geometric configurations facilitating unidirectional block and reentry. Physica D 1992;59:275–296.
68. Rohr S, Salzberg RM. Characterization of impulse propagation at the microscopic level across geometrically defined expansions of excitable tissues: multiple site optical recording of transmembrane voltage (MSORTV) in patterned growth heart cell cultures. J Gen Physiol 1994;104:287–309.
69. Fast VG, Kleber AG. Block of impulse propagation at an abrupt tissue expansion: evaluation of the critical strand diameter in 2- and 3-dimensional computer models. Cardiovasc Res 1995;30:449–459.
70. Cabo C, Pertsov AM, Baxter WT, Davidenko JM, Gray RA, Jalife J. Wave-front curvature as a cause of slow conduction and block in isolated cardiac muscle. Circ Res 1994;75:1014–1028.
71. Kléber AG, Rudy Y. Basic mechanisms of cardiac impulse propagation and associated arrhythmias. Physiol Rev 2004;84:431–488.
72. Ciaccio EJ, Ashikaga H, Kaba RA, et al. Model of reentrant ventricular tachycardia based on infarct border zone geometry predicts reentrant circuit features as determined by activation mapping. Heart Rhythm 2007;4:1034–1045.
73. Ciaccio EJ, Coromilas J, Ashikaga H, et al. Model of unidirectional block formation leading to reentrant ventricular tachycardia in the infarct border zone of postinfarction canine hearts. Comput Biol Med 2015;62:254–263.
74. Ciaccio EJ, Coromilas J, Wit AL, Peters NS, Garan H. Formation of reentrant circuits in the mid-myocardial infarct border zone. Comput Biol Med 2016; 71:205–213.
75. Ciaccio EJ, Coromilas J, Wit AL, Peters NS, Garan H. Formation of functional conduction block during the onset of reentrant ventricular tachycardia. Circ Arrhythm Electrophysiol 2016;9:e004462.
76. Brunckhorst CB, Delacretaz E, Soejima K, Maisel WH, Friedman PL, Stevenson WG. Identification of the ventricular tachycardia isthmus after infarction by pace mapping. Circulation 2004;110:652–659.
77. Ciaccio EJ, Costeas C, Coromilas J, Wit AL. Static relationship of cycle length to reentrant circuit geometry. Circulation 2001;104:1946–1951.
78. Ciaccio EJ. Localization of the slow conduction zone during reentrant ventricular tachycardia. Circulation 2000;102:464–469.
79. Ciaccio EJ. Dynamic relationship of cycle length to reentrant circuit geometry and to the slow conduction zone during ventricular tachycardia. Circulation 2001;103:1017–1024.
80. Rottmann M, Kleber AG, Barkagan M, et al. Activation during sinus rhythm in ventricles with healed infarction: differentiation between arrhythmogenic and nonarrhythmogenic scar. Circ Arrhythm Electrophysiol 2019;12:e007879.
81. Nishimura T, Upadhyay GA, Aziz ZA, et al. Circuit determinants of ventricular tachycardia cycle length: characterization of fast and unstable human ventricular tachycardia. Circulation 2021;143:212–226.
82. Sasaki T, Miller CF, Hansford R, et al. Impact of nonischemic scar features on local ventricular electrograms and scar-related ventricular tachycardia circuits in patients with nonischemic cardiomyopathy. Circ Arrhythm Electrophysiol 2013;6:1139–1147.
83. Takigawa M, Duchateau J, Sacher F, et al. Are wall thickness channels defined by computed tomography predictive of isthmuses of postinfarction ventricular tachycardia? Heart Rhythm 2019;16:1661–1668.
84. Kocovic DZ, Harada T, Friedman PL, Stevenson WG. Characteristics of electrograms recorded at reentry circuit sites and bystanders during ventricular tachycardia after myocardial infarction. J Am Coll Cardiol 1999; 34:381–388.
85. de Chillou C, Lacroix D, Klug D, et al. Isthmus characteristics of reentrant ventricular tachycardia after myocardial infarction. Circulation 2002;105:726–731.
86. Soejima K, Stevenson WG, Maisel WH, Sapp JL, Epstein LM. Electrically unexcitable scar mapping based on pacing threshold for identification of the reentry circuit isthmus: feasibility for guiding ventricular tachycardia ablation. Circulation 2002;106:1678–1683.
87. Komatsu Y, Cochet H, Jadidi A, et al. Regional myocardial wall thinning at multidetector computed tomography correlates to arrhythmogenic substrate in postinfarction ventricular tachycardia: assessment of structural and electrical substrate. Circ Arrhythm Electrophysiol 2013;6:342–350.
88. Spach MS, Miller WT III, Miller-Jones E, Warren RB, Barr RC. Extracellular potentials related to intracellular action potentials during impulse conduction in anisotropic canine cardiac muscle. Circ Res 1979;45:188–204.
89. Ciaccio EJ, Ashikaga H, Coromilas J, et al. Model of bipolar electrogram fractionation and conduction block associated with activation wavefront direction at infarct border zone lateral isthmus boundaries. Circ Arrhythm Electrophysiol 2014;7:152–163.
90. Anter E, Duytschaever M, Shen C, et al. Activation mapping with integration of vector and velocity information improves the ability to identify the mechanism and location of complex scar-related atrial tachycardias. Circ Arrhythm Electrophysiol 2018;11:e006536.
91. Cheung JW. Targeting abnormal electrograms for substrate-based ablation of ventricular tachycardia: can we ablate smarter? JACC Clin Electrophysiol 2020;6:812–814.
92. Soejima K, Suzuki M, Maisel WH, et al. Catheter ablation in patients with multiple and unstable ventricular tachycardias after myocardial infarction: short ablation lines guided by reentry circuit isthmuses and sinus rhythm mapping. Circulation 2001;104:664–669.
93. Stevenson WG. Catheter ablation of monomorphic ventricular tachycardia. Curr Opin Cardiol 2005;20:42–47.
94. Stevenson WG, Soejima K. Catheter ablation for ventricular tachycardia. Circulation 2007;115:2750–2760.
95. Garan H, Ruskin JN. Reproducible termination of ventricular tachycardia by a single extrastimulus within the reentry circuit during the ventricular effective refractory period. Am Heart J 1988;116:546–550.
96. Harada T, Stevenson WG, Kocovic DZ, Friedman PL. Catheter ablation of ventricular tachycardia after myocardial infarction: relation of endocardial sinus rhythm late potentials to the reentry circuit. J Am Coll Cardiol 1997; 30:1015–1023.
97. de Bakker JM, van Capelle FJ, Janse MJ, et al. Macroreentry in the infarcted human heart: the mechanism of ventricular tachycardias with a "focal" activation pattern. J Am Coll Cardiol 1991;18:1005–1014.
98. Ciaccio EJ, Tosti AC, Scheinman MM. Relationship between sinus rhythm activation and the reentrant ventricular tachycardia isthmus. Circulation 2001; 104:613–619.
99. Zhang J, Cooper DH, Desouza KA, et al. Electrophysiologic scar substrate in relation to VT: noninvasive high-resolution mapping and risk assessment with ECGI. Pacing Clin Electrophysiol 2016;39:781–791.
100. Lin CY, Silberbauer J, Lin YJ, et al. Simultaneous amplitude frequency electrogram transformation (SAFE-T) mapping to identify ventricular tachycardia arrhythmogenic potentials in sinus rhythm. JACC Clin Electrophysiol 2016; 2:459–470.
101. Josephson ME, Anter E. Substrate mapping for ventricular tachycardia: assumptions and misconceptions. JACC Clin Electrophysiol 2015;1:341–352.
102. Tzou WS, Frankel DS, Hegeman T, et al. Core isolation of critical arrhythmia elements for treatment of multiple scar-based ventricular tachycardias. Circ Arrhythm Electrophysiol 2015;8:353–361.
103. de Bakker JM, Wittkampf FH. The pathophysiologic basis of fractionated and complex electrograms and the impact of recording techniques on their detection and interpretation. Circ Arrhythm Electrophysiol 2010;3:204–213.
104. Campos FO, Orini M, Arnold R, et al. Assessing the ability of substrate mapping techniques to guide ventricular tachycardia ablation using computational modelling. Comput Biol Med 2021;130:104214.
105. Martin CA, Martin R, Maury P, et al. Effect of activation wavefront on electrogram characteristics during ventricular tachycardia ablation. Circ Arrhythm Electrophysiol 2019;12:e007293.
106. Ciaccio EJ, Scheinman MM, Fridman V, Schmitt H, Coromilas J, Wit AL. Dynamic changes in electrogram morphology at functional lines of block in reentrant circuits during ventricular tachycardia in the infarcted canine heart: a new method to localize reentrant circuits from electrogram features using adaptive template matching. J Cardiovasc Electrophysiol 1999;10:194–213.
107. Ciaccio EJ, Scheinman MM, Wit AL. Relationship of specific electrogram characteristics during sinus rhythm and ventricular pacing determined by adaptive template matching to the location of functional reentrant circuits that cause ventricular tachycardia in the infarcted canine heart. J Cardiovasc Electrophysiol 2000;11:446–457.
108. Dillon S, Ursell PC, Wit AL. Pseudo block caused by anisotropic conduction: a new mechanism for sustained reentry. (Abstract) Circulation 1985;72:III–279.
109. Miller JM, Kienzle MG, Harken AH, Josephson ME. Morphologically distinct sustained ventricular tachycardias in coronary artery disease: significance and surgical results. J Am Coll Cardiol 1984;4:1073–1079.

110. Wilber D, Davis MJ, Rosenbaum M, Ruskin JN, Garan H. Incidence and determinants of multiple morphologically distinct sustained ventricular tachycardias. J Am Coll Cardiol 1987;10:583–591.
111. Buxton AE, Waxman HL, Marchlinski FE, Untereker WJ, Waspe LE, Josephson ME. Role of triple extrastimuli during electrophysiologic study of patients with documented sustained ventricular tachyarrhythmias. Circulation 1984;69:532–540.
112. Mitrani RD, Biblo LA, Carlson MD, Gatzoylis KA, Henthorn RW, Waldo AL. Multiple monomorphic ventricular tachycardia configurations predict failure of antiarrhythmic drug therapy guided by electrophysiologic study. J Am Coll Cardiol 1993;22:1117–1122.
113. Trappe HJ, Klein H, Auricchio A, Wenzlaff P, Lichtlen PR. Catheter ablation of ventricular tachycardia: role of the underlying etiology and the site of energy delivery. Pacing Clin Electrophysiol 1992;15:411–424.
114. Kim YH, Guillermo S, Trouton TG, et al. Treatment of ventricular tachycardia by transcatheter radiofrequency ablation in patients with ischemic heart disease. Circulation 1994;89:1094–1102.
115. Tung R, Boyle NG, Shivkumar K. Catheter ablation of ventricular tachycardia. Circulation 2010;122:e389–e391.
116. Ciaccio EJ, Coromilas J, Costeas CA, Wit AL. Sinus rhythm electrogram shape measurements are predictive of the origins and characteristics of multiple reentrant ventricular tachycardia morphologies. J Cardiovasc Electrophysiol 2004; 15:1293–1301.
117. Gough WB, Mehra R, Restivo M, Zeiler RH, el-Sherif N. Reentrant ventricular arrhythmias in the late myocardial infarction period in the dog. 13: correlation of activation and refractory maps. Circ Res 1985;57:432–442.
118. Estner HL, Zviman MM, Herzka D, et al. The critical isthmus sites of ischemic ventricular tachycardia are in zones of tissue heterogeneity, visualized by magnetic resonance imaging. Heart Rhythm 2011;8:1942–1949.
119. Costeas C, Peters NS, Waldecker B, Ciaccio EJ, Wit AL, Coromilas J. Mechanisms causing sustained ventricular tachycardia with multiple QRS morphologies: results of mapping studies in the infarcted canine heart. Circulation 1997;96:3721–3731.
120. Della Bella P, Riva S, Fassini G, et al. Incidence and significance of pleomorphism in patients with postmyocardial infarction ventricular tachycardia. Acute and long-term outcome of radiofrequency catheter ablation. Eur Heart J 2004; 25:1127–1138.
121. Waspe LE, Brodman R, Kim SG, et al. Activation mapping in patients with coronary artery disease with multiple ventricular tachycardia configurations: occurrence and therapeutic implications of widely separate sites of origin. J Am Coll Cardiol 1985;5:1075–1086.
122. Josephson ME, Horowitz LN, Farshidi AR, Spielman SR, Michelson EL, Greenspan AM. Recurrent sustained ventricular tachycardia. 4. Pleomorphism. Circulation 1979;59:459–468.
123. Bogun F, LI YG, Groenefeld G, et al. Prevalence of a shared isthmus in postinfarction patients with pleiomorphic, hemodynamically tolerated ventricular tachycardias. J Cardiovasc Electrophysiol 2002;13:237–241.
124. Liu E, Josephson ME. Pleomorphic ventricular tachycardia and risk for sudden cardiac death. Circ Arrhythm Electrophysiol 2011;4:2–4.
125. Hadid C, Almendral J, Ortiz M, et al. Incidence, determinants, and prognostic implications of true pleomorphism of ventricular tachycardia in patients with implantable cardioverter-defibrillators: a substudy of the DATAS Trial. Circ Arrhythm Electrophysiol 2011;4:33–42.
126. El-Sherif N, Mehra R, Gough WB, Zeiler RH. Reentrant ventricular arrhythmias in the late myocardial infarction period: interruption of reentrant circuits by cryothermal techniques. Circulation 1983;8:644–653.
127. Garan H, Ruskin JN. Localized reentry: mechanism of induced sustained ventricular tachycardia in canine model of myocardial infarction. J Clin Invest 1984;74:377–392.
128. Berger MD, Waxman HL, Buxton AE, Marchlinski FE, Josephson ME. Spontaneous compared with induced onset of sustained ventricular tachycardia. Circulation 1988;78:885–892.
129. Pogwizd SM, Corr PB. Reentrant and nonreentrant mechanisms contribute to arrhythmogenesis during early myocardial ischemia: results using three-dimensional mapping. Circ Res 1987;61:352–371.
130. Quan W, Rudy Y. Unidirectional block and reentry of cardiac excitation: a model study. Circ Res 1990;66:367–382.
131. Dukkipati SR, Choudry S, Koruth JS, Miller MA, Whang W, Reddy VY. Catheter ablation of ventricular tachycardia in structurally normal hearts: indications, strategies, and outcomes—part I. J Am Coll Cardiol 2017;70:2909–2923.
132. Roberts DE, Herse LT, Scher AM. Influence of cardiac fiber orientation on wavefront voltage, conduction velocity, and tissue resistivity in the dog. Circ Res 1979;44:701–712.
133. Spach MS, Miller WT 3rd, Geselowitz DB, Barr RC, Kootsey JM, Johnson EA. The discontinuous nature of propagation in normal canine cardiac muscle. Evidence for recurrent discontinuities of intracellular resistance that affect the membrane currents. Circ Res 1981;48:39–54.
134. Antzelevitch C, Burashnikov A. Overview of basic mechanisms of cardiac arrhythmia. Card Electrophysiol Clin 2011;3:23–45.
135. El-Sherif N. The figure 8 model of reentrant excitation in the canine post infarction heart. In: Zipes DP, Jalife J, eds. Cardiac Electrophysiology and Arrhythmias. New York: Grune & Stratton; 1985 p. 363–378.
136. Spach MS, Josephson ME. Initiating reentry: the role of nonuniform anisotropy in small circuits. J. Cardiovasc Electrophysiol 1994; 5:182–209.
137. Wit AL. Remodeling of cardiac gap junctions: the relationship to the genesis of ventricular tachycardia. J Electrocardiol 2001;34(Suppl):77–83.
138. Costa CM, Plank G, Rinaldi CA, Niederer SA, Bishop MJ. Modeling the electrophysiological properties of the infarct border zone. Front Physiol 2018;9:356.
139. Spach MS, Dolber PC, Heidlage JF. Influence of the passive anisotropic properties on directional differences in propagation following modification of the sodium conductance in human atrial muscle. A model of reentry based on anisotropic discontinuous propagation. Circ Res 1988;62:811–832.
140. Saffitz JE, Kléber AG. Gap junctions, slow conduction, and ventricular tachycardia after myocardial infarction. J Am Coll Cardiol 2012; 60:1111–1113.
141. Tanner H, Hindricks G, Volkmer M, et al. Catheter ablation of recurrent scar-related ventricular tachycardia using electroanatomical mapping and irrigated ablation technology: results of the prospective multicenter Euro-VT-study. J Cardiovasc Electrophysiol 2010;21:47–53.
142. Tung R, Vaseghi M, Frankel DS, et al. Freedom from recurrent ventricular tachycardia after catheter ablation is associated with improved survival in patients with structural heart disease: an International VT Ablation Center Collaborative Group study. Heart Rhythm 2015;12:1997–2007.
143. Viswanathan K, Mantziari L, Butcher C, et al. Evaluation of a novel high-resolution mapping system for catheter ablation of ventricular arrhythmias. Heart Rhythm 2017;14:176–183.
144. Tanaka Y, Genet M, Lee LC, Martin AJ, Sievers R, Gerstenfeld EP. Utility of high-resolution electroanatomic mapping of the left ventricle using a multispline basket catheter in a swine model of chronic myocardial infarction. Heart Rhythm 2015;12:144–154.
145. Thajudeen A, Jackman WM, Stewart B, et al. Correlation of scar in cardiac MRI and high-resolution contact mapping of left ventricle in a chronic infarct model. Pacing Clin Electrophysiol 2015;38:663–674.
146. Josephson ME, Harken AH, Horowitz LN. Endocardial excision: a new surgical technique for the treatment of recurrent ventricular tachycardia. Circulation 1979;60:1430–1439.
147. Kaltenbrunner W, Cardinal R, Dubuc M, et al. Epicardial and endocardial mapping of ventricular tachycardia in patients with myocardial infarction. Is the origin of the tachycardia always subendocardially localized? Circulation 1991; 84:1058–1071.
148. Bhaskaran A, Nayyar S, Porta-Sánchez A, et al. Direct and indirect mapping of intramural space in ventricular tachycardia. Heart Rhythm 2020; 17:439–446.
149. AbdelWahab A, Stevenson W, Thompson K, et al. Intramural ventricular recording and pacing in patients with refractory ventricular tachycardia: initial findings and feasibility with a retractable needle catheter. Circ Arrhythm Electrophysiol 2015;8:1181–1188.
150. Tian J, Jeudy J, Smith MF, et al. Three-dimensional contrast-enhanced multidetector CT for anatomic, dynamic, and perfusion characterization of abnormal myocardium to guide ventricular tachycardia ablations. Circ Arrhythm Electrophysiol 2010;3:496–504.
151. Treibel TA, White SK, Moon JC. Myocardial tissue characterization: histological and pathophysiological correlation. Curr Cardiovasc Imaging Rep 2014; 7:1–9.
152. Kim RJ, Fieno DS, Parrish TB, et al. Relationship of MRI delayed contrast enhancement to irreversible injury, infarct age, and contractile function. Circulation 1999;100:1992–2002.
153. Setser RM, Bexell DG, O'Donnell TP, et al. Quantitative assessment of myocardial scar in delayed enhancement magnetic resonance imaging. J Magn Reson Imaging 2003;18:434–441.
154. Gerstenfeld EP, Desjardins BE, Haqqani H, et al. Correlation of bipolar voltage mapping and delayed enhancement MRI for detecting myocardial scar in a chronic ovine infarct model. Heart Rhythm 2011;8:S92–S93.
155. O'Hanlon R, Grasso A, Roughton M, et al. Prognostic significance of myocardial fibrosis in hypertrophic cardiomyopathy. J Am Coll Cardiol 2010; 56:867–874.
156. Assomull RG, Prasad SK, Lyne J, et al. Cardiovascular magnetic resonance, fibrosis, and prognosis in dilated cardiomyopathy. J Am Coll Cardiol 2006; 48:1977–1985.

157. Schmidt A, Azevedo CF, Cheng A, et al. Infarct tissue heterogeneity by magnetic resonance imaging identifies enhanced cardiac arrhythmia susceptibility in patients with left ventricular dysfunction. Circulation 2007;115:2006–2014.
158. Kwon DH, Asamoto L, Popovic ZB, et al. Infarct characterization by delayed enhancement cardiac magnetic resonance imaging is a powerful independent and incremental predictor of mortality in patients with advanced ischemic cardiomyopathy. Circ Cardiovasc Imaging 2015;7:796–804.
159. Chen Z, Sohal M, Voigt T, et al. Myocardial tissue characterization by cardiac magnetic resonance imaging using T1 mapping predicts ventricular arrhythmia in ischemic and non–ischemic cardiomyopathy patients with implantable cardioverter-defibrillators. Heart Rhythm 2015;12:792–801.
160. Takigawa M, Martin R, Cheniti G, et al. Detailed comparison between the wall thickness and voltages in chronic myocardial infarction. J Cardiovasc Electrophysiol 2019;30:195–204.
161. Alyesh DM, Siontis KC, Sharaf Dabbagh G, et al. Postinfarction myocardial calcifications on cardiac computed tomography: implications for mapping and ablation in patients with nontolerated ventricular tachycardias. Circ Arrhythm Electrophysiol 2019;12:e007023.
162. Salerno M, Sharif B, Arheden H, et al. Recent advances in cardiovascular magnetic resonance: techniques and applications. Circ Cardiovasc Imaging 2017;10:e003951.
163. Tung R, Josephson ME, Bradfield JS, Shivkumar K. Directional influences of ventricular activation on myocardial scar characterization: voltage mapping with multiple wavefronts during ventricular tachycardia ablation. Circ Arrhythm Electrophysiol 2016;9:e004155.
164. Jaïs P, Maury P, Khairy P, et al. Elimination of local abnormal ventricular activities: a new end point for substrate modification in patients with scar-related ventricular tachycardia. Circulation 2012;125:2184–2196.
165. Vergara P, Trevisi N, Ricco A, et al. Late potentials abolition as an additional technique for reduction of arrhythmia recurrence in scar related ventricular tachycardia ablation. J Cardiovasc Electrophysiol 2012;23:621–627.
166. Di Biase L, Burkhardt JD, Lakkireddy D, et al. Ablation of stable VTs versus substrate ablation in ischemic cardiomyopathy: the VISTA randomized multicenter trial. J Am Coll Cardiol 2015;66:2872–2882.
167. Gökoğlan Y, Mohanty S, Gianni C, et al. Scar homogenization versus limited-substrate ablation in patients with nonischemic cardiomyopathy and ventricular tachycardia. J Am Coll Cardiol 2016;68:1990–1998.
168. Yoshida K, Sekiguchi Y, Tanoue K, et al. Feasibility of targeting catheter ablation to the markedly low-voltage area surrounding infarct scars in patients with post-infarction ventricular tachycardia. Circ J 2008;72:1112–1119.
169. Sramko M, Abdel-Kafi S, van der Geest RJ, et al. New adjusted cutoffs for "normal" endocardial voltages in patients with post-infarct LV remodeling. JACC Clin Electrophysiol 2019;5:1115–1126.
170. Berte B, Zeppenfeld K, Tung R. Impact of micro-, mini- and multi-electrode mapping on ventricular substrate characterisation. Arrhythm Electrophysiol Rev 2020;9:128–135.
171. Takigawa M, Relan J, et al. Effect of bipolar electrode orientation on local electrogram properties. Heart Rhythm 2018;15:1853–1861.
172. Anter E, Josephson ME. Bipolar voltage amplitude: what does it really mean? Heart Rhythm 2016;13:326–327.
173. Okubo K, Frontera A, Bisceglia C, et al. Grid mapping catheter for ventricular tachycardia ablation. Circ Arrhythm Electrophysiol 2019;12:e007500.
174. Sacher F, Lim HS, Derval N, et al. Substrate mapping and ablation for ventricular tachycardia: the LAVA approach. J Cardiovasc Electrophysiol 2015;26:464–471.
175. Codreanu A, Odille F, Aliot E, et al. Electroanatomic characterization of post-infarct scars: comparison with 3-dimensional myocardial scar reconstruction based on magnetic resonance imaging. J Am Coll Cardiol 2008;52:839–842.
176. Bradfield JS, Tung R, Shivkumar K. Transmural "scar-to-scar" reentrant ventricular tachycardia. Indian Pacing Electrophysiol J 2013;13:212–216.
177. Bogun FM, Desjardins B, Good E, et al. Delayed-enhanced magnetic resonance imaging in nonischemic cardiomyopathy: utility for identifying the ventricular arrhythmia substrate. J Am Coll Cardiol 2009;53:1138–1145.
178. Dukkipati SR, Koruth JS, Choudry S, Miller MA, Whang W, Reddy VY. Catheter ablation of ventricular tachycardia in structural heart disease: indications, strategies, and outcomes—part II. J Am Coll Cardiol 2017;70:2924–2941.
179. Cuculich PS, Schill MR, Kashani R, et al. Noninvasive cardiac radiation for ablation of ventricular tachycardia. N Engl J Med 2017;377:2325–2336.
180. Jiang R, Beaser AD, Aziz Z, Upadhyay GA, Nayak HM, Tung R. High-density grid catheter for detailed mapping of sinus rhythm and scar-related ventricular tachycardia: comparison with a linear duodecapolar catheter. JACC Clin Electrophysiol 2020;6:311–323.
181. Cantwell CD, Roney CH, Ng FS, Siggers JH, Sherwin SJ, Peters NS. Techniques for automated local activation time annotation and conduction velocity estimation in cardiac mapping. Comput Biol Med 2015;65:229–242.
182. Irie T, Yu R, Bradfield JS, et al. Relationship between sinus rhythm late activation zones and critical sites for scar-related ventricular tachycardia: systematic analysis of isochronal late activation mapping. Circ Arrhythm Electrophysiol 2015;8:390–399.
183. de Jong S, van Veen TA, van Rijen HV, de Bakker JM. Fibrosis and cardiac arrhythmias. J Cardiovasc Pharmacol 2011;57:630–638.
184. Aziz Z, Shatz D, Raiman M, et al. Targeted ablation of ventricular tachycardia guided by wavefront discontinuities during sinus rhythm: a new functional substrate mapping strategy. Circulation 2019;140:1383–1397.
185. Jackson N, Gizurarson S, Viswanathan K, et al. Decrement evoked potential mapping: basis of a mechanistic strategy for ventricular tachycardia ablation. Circ Arrhythm Electrophysiol 2015;8:1433–1442.
186. Porta-Sánchez A, Jackson N, Lukac P, et al. Multicenter study of ischemic ventricular tachycardia ablation with decrement-evoked potential (DEEP) mapping with extra stimulus. JACC Clin Electrophysiol 2018;4:307–315.
187. de Riva M, Naruse Y, Ebert M, et al. Targeting the hidden substrate unmasked by right ventricular extrastimulation improves ventricular tachycardia ablation outcome after myocardial infarction. JACC Clin Electrophysiol 2018;4:316–327.
188. Hadjis A, Frontera A, Limite LR, et al. Complete electroanatomic imaging of the diastolic pathway is associated with improved freedom from ventricular tachycardia recurrence. Circ Arrhythm Electrophysiol 2020;13:e008651.
189. Proietti R, Lichelli L, Lellouche N, Dhanjal T. The challenge of optimising ablation lesions in catheter ablation of ventricular tachycardia. J Arrhythm 2020;37:140–147.
190. Anter E. Limitations and pitfalls of substrate mapping for ventricular tachycardia. JACC Clin Electrophysiol 2021;7:542–560.